Free Radical Biology and Medicine 226 (2025) 408–420

Contents lists available at ScienceDirect

Free Radical Biology and Medicine

journal homepage: www.elsevier.com/locate/freeradbiomed

Tsa1 is the dominant peroxide scavenger and a source of H_2O_2-dependent GSSG production in yeast

Jannik Zimmermann [a], Lukas Lang [b], Gaetano Calabrese [c], Hugo Laporte [a], Prince S. Amponsah [a,d], Christoph Michalk [d], Tobias Sukmann [a], Julian Oestreicher [a], Anja Tursch [e], Esra Peker [c], Theresa N.E. Owusu [e], Matthias Weith [c], Leticia Prates Roma [f], Marcel Deponte [b,**], Jan Riemer [c,g,***], Bruce Morgan [a,*]

[a] Institute of Biochemistry, Centre for Human and Molecular Biology (ZHMB), Saarland University, 66123, Saarbrücken, Germany
[b] Faculty of Chemistry, Comparative Biochemistry, RPTU Kaiserslautern, D-67663, Kaiserslautern, Germany
[c] Institute for Biochemistry, Redox Biochemistry, University of Cologne, Zuelpicher Str. 47a/R. 3.49, 50674, Cologne, Germany
[d] Cellular Biochemistry, RPTU Kaiserslautern, 67663, Kaiserslautern, Germany
[e] Division of Redox Regulation, DKFZ-ZMBH Alliance, German Cancer Research Center (DKFZ), Im Neuenheimer Feld 280, 69120, Heidelberg, Germany
[f] Institute of Biophysics, Centre for Human and Molecular Biology (ZHMB), Saarland University, 66424, Homburg, Germany
[g] Cologne Excellence Cluster on Cellular Stress Responses in Aging-Associated Diseases (CECAD), University of Cologne, 50931, Cologne, Germany

ARTICLE INFO

Keywords:
roGFP2
HyPer7
Peroxiredoxin
Catalase
Thiol peroxidase
Heme peroxidase
H_2O_2 scavenging

ABSTRACT

Hydrogen peroxide (H_2O_2) is an important biological molecule, functioning both as a second messenger in cell signaling and, especially at higher concentrations, as a cause of cell damage. Cells harbor multiple enzymes that have peroxide reducing activity *in vitro*. However, the contribution of each of these enzymes towards peroxide scavenging *in vivo* is less clear. Therefore, to directly investigate *in vivo* peroxide scavenging, we used the genetically encoded peroxide probes, roGFP2-Tsa2ΔC$_R$ and HyPer7, to systematically screen the peroxide scavenging capacity of baker's yeast thiol and heme peroxidase mutants. We show that the 2-Cys peroxiredoxin Tsa1 alone is responsible for almost all exogenous H_2O_2 and *tert*-butyl hydroperoxide scavenging. Furthermore, Tsa1 can become an important source of H_2O_2-dependent cytosolic glutathione disulfide production. The two catalases and cytochrome *c* peroxidase only produce observable scavenging defects at higher H_2O_2 concentrations when these three heme peroxidases are removed in combination. We also analyzed the reduction of Tsa1 *in vitro*, revealing that the enzyme is efficiently reduced by thioredoxin-1 with a rate constant of 2.8×10^6 $M^{-1}s^{-1}$ but not by glutaredoxin-2. Tsa1 reduction by reduced glutathione occurs nonenzymatically with a rate constant of 2.9 $M^{-1}s^{-1}$. Hence, the observed Tsa1-dependent glutathione disulfide production in yeast probably requires the oxidation of thioredoxins. Our findings clarify the importance of the various thiol and heme peroxidases for peroxide removal and suggest that most thiol peroxidases have alternative or specialized functions in specific subcellular compartments.

1. Introduction

Hydrogen peroxide (H_2O_2) is an important cellular redox molecule. It has multiple cellular sources, including several enzymes that appear to be dedicated to the direct or indirect production of H_2O_2. Whilst it is now well understood that H_2O_2 can function as a second messenger in cellular signaling, it is also unequivocal that beyond a certain threshold, H_2O_2 is toxic to cells and can readily lead to cell death [1,2]. In the context of both signaling and toxicity it is likely crucial for cells to tightly control H_2O_2 levels.

Cells harbor a range of H_2O_2 scavenging enzymes, including thiol- or selenol-dependent peroxidases, for example, peroxiredoxins and glutathione peroxidases, as well as heme peroxidases such as catalases and cytochrome *c* peroxidases [3–6]. Nonetheless, whilst many

* Corresponding author. Institute of Biochemistry, Centre for Human and Molecular Biology (ZHMB), Saarland University, 66123, Saarbrücken, Germany.
** Corresponding author. Faculty of Chemistry, Comparative Biochemistry, RPTU Kaiserslautern, D-67663, Kaiserslautern, Germany.
*** Corresponding author. Institute for Biochemistry, Redox Biochemistry, University of Cologne, Zuelpicher Str. 47a/R. 3.49, 50674, Cologne, Germany.
E-mail addresses: deponte@chemie.uni-kl.de (M. Deponte), jan.riemer@uni-koeln.de (J. Riemer), bruce.morgan@uni-saarland.de (B. Morgan).

https://doi.org/10.1016/j.freeradbiomed.2024.11.004
Received 3 September 2024; Received in revised form 30 October 2024; Accepted 2 November 2024
Available online 6 November 2024

enzymes can efficiently reduce H_2O_2 *in vitro*, the contribution of a specific enzyme towards the total cellular H_2O_2 scavenging capacity is often less clear. It will depend upon the expression level of the according gene, the subcellular compartment, and the enzymatic activity relative to other H_2O_2 reactive enzymes present [7]. Furthermore, the relevance of a particular H_2O_2 scavenging enzyme may change dynamically over time in response to changing environmental conditions, including carbon source, culture growth phase and culture density, previous exposure to compounds including oxidants, electrophiles and heavy metals, and potentially even illumination [8–11].

Budding yeast, *Saccharomyces cerevisiae*, harbor five peroxiredoxins, three glutathione peroxidase-like enzymes, two catalases and one cytochrome *c* peroxidase. The typical 2-Cys peroxiredoxin, Tsa1, is the most abundant peroxidase in *S. cerevisiae* [12,13] and several studies have concluded that Tsa1 is the dominant H_2O_2 scavenging enzyme in this organism [14–19]. However, these studies all relied on *indirect* assays, for example, by correlating cell growth, cell death or genomic stability to peroxide treatments [14–18,20–28]. It is frequently assumed that a difference in the sensitivity of a specific mutant strain towards H_2O_2, or other peroxides, is indicative of a change in the peroxide scavenging capacity of that mutant compared to wild-type cells. The validity of this approach depends upon the *assumption* that decreased H_2O_2 scavenging capacity always leads to increased sensitivity towards H_2O_2-induced growth arrest or cell death. However, thiol and selenol peroxidases have multiple cellular functions alongside peroxide detoxification, including H_2O_2-dependent signal transduction [3,4,28,29], chaperone activity [30,31] and moonlighting functions such as the formation of the mitochondrial capsule of sperm cells [32]. Conceivably, disruption of these alternative functions could underlie growth impairment or changes in genomic stability in different peroxidase mutants. In line with this hypothesis, mis-regulation of protein kinase A (PKA) signaling — not impaired H_2O_2 scavenging — was proposed to underlie the sensitivity of *TSA1* knockout yeast cells to H_2O_2-induced cell death [33]. Furthermore, peroxide scavenging capacity and sensitivity to peroxide-induced cell death can be readily uncoupled. For example, it has been reported that depletion of pools of reduced thioredoxins or glutathione (GSH) (and the accumulation of oxidized thioredoxins or glutathione disulfide) may be important mediators of H_2O_2 toxicity [34–38]. In this scenario, inactivation of peroxiredoxin activity is even beneficial for cell survival under peroxide challenges [34,35]. Finally, although Tsa1 is extremely abundant, peroxiredoxin activity may be limited by numerous factors such as post-translational modification [39–41], including hyperoxidation [42], and by the supply of electrons. For example, the thioredoxin reductase level was recently reported as an important determinant of cellular H_2O_2 scavenging capacity [43].

Taken together, recent experimental observations and theoretical considerations, prompted us to explicitly test the relative contribution of the various thiol and heme peroxidases in *S. cerevisiae* towards total cellular peroxide scavenging capacity. In contrast to indirect growth assays, we *directly* and *quantitatively* analyzed the peroxide scavenging capacity of deletion and overexpression mutants using two ultra-sensitive, genetically encoded H_2O_2 probes, roGFP2-Tsa2ΔC_R [44] and HyPer7 [45], that were localized to the mitochondrial matrix and cytosol, respectively. We found that the typical 2-Cys peroxiredoxin Tsa1 is the major scavenger of both H_2O_2 and *tert*-butyl hydroperoxide (*t*-BuOOH) in fermentative and respiratory conditions and efficiently outcompetes all other endogenous cellular thiols for H_2O_2 including the reactive thiol on the ultra-sensitive H_2O_2 probe, HyPer7. Regarding heme peroxidases, the two yeast catalases only have a noticeable impact on cellular H_2O_2 scavenging at higher H_2O_2 concentrations and, even then, only when the encoding genes are simultaneously deleted in combination with a deletion of the gene encoding cytochrome *c* peroxidase. Finally, we analyzed the reduction of Tsa1 *in vitro* and in yeast, revealing that the enzyme is efficiently reduced by thioredoxin 1 (Trx1) but can become a major source of H_2O_2-dependent glutathione disulfide (GSSG) production when thioredoxins are oxidized, which has been shown to readily occur under peroxide challenge in other yeast [35,46].

2. Results

2.1. Tsa1 is the major scavenger of cellular peroxide

We first sought to directly quantify the capacity of the yeast cytosol to eliminate H_2O_2 and *t*-BuOOH and to define a 'hierarchy of importance' of the different peroxide removing enzymes. To this end, we utilized an assay that we have previously developed in which the sensitivity of the response of a mitochondrial-localized roGFP2-Tsa2ΔC_R probe (Su9-roGFP2-Tsa2ΔC_R) to exogenously applied peroxide serves as a proxy for the H_2O_2 scavenging capacity of the cytosol [34,44]. The magnitude of the probe response is dependent upon the quantity of exogenous peroxide that reaches the matrix and thus is inversely dependent upon the peroxide scavenging capacity of the cytosol

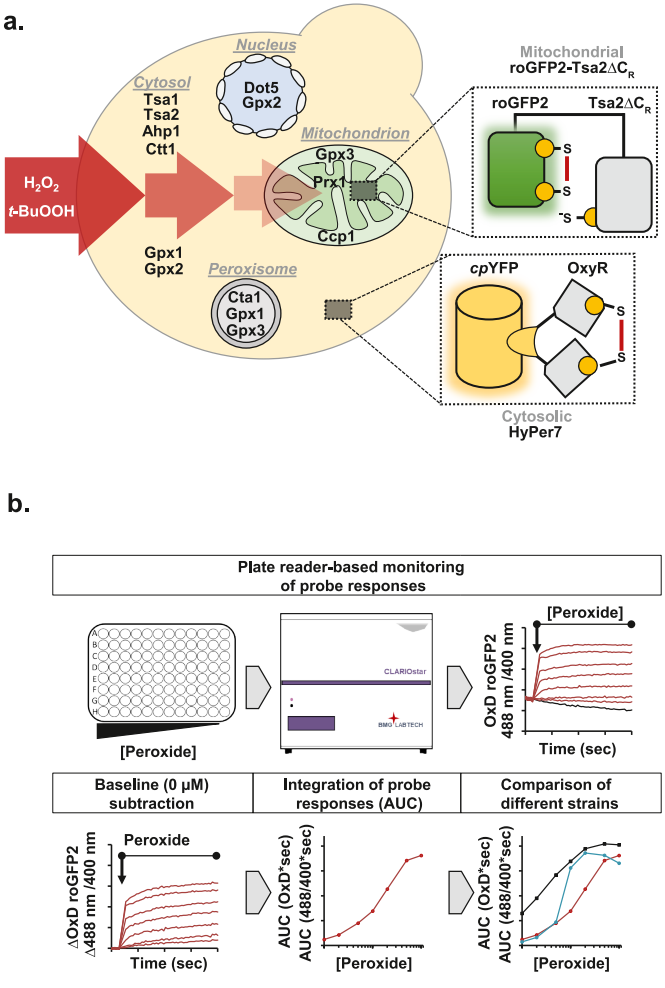

Fig. 1. Development of an assay for monitoring cytosolic peroxide scavenging capacity.
a. Schematic illustration of the experimental setup. A matrix localized, ultra-sensitive, Su9-roGFP2-Tsa2ΔC_R peroxide probe, was expressed in strains deleted for or overexpressing the genes encoding the various thiol peroxidases, catalases and cytochrome *c* peroxidase, either individually or in combination. The response of the Su9-roGFP2-Tsa2ΔC_R probe is dependent upon the quantity of peroxide that can diffuse through the cytosol, which in turn, is inversely dependent upon the peroxide scavenging capacity. Therefore, the sensitivity of the Su9-roGFP2-Tsa2ΔC_R probe response is inversely dependent upon the cellular peroxide scavenging capacity. **b.** Su9-roGFP2-Tsa2ΔC_R probe responses were analyzed by calculating the integrated area under the curve (A.U.C.) of the untreated baseline corrected response between 0 and 2000 s.

(Fig. 1a). Baker's yeast harbors five peroxiredoxins, including the highly abundant Prx1-type typical 2-Cys peroxiredoxin, Tsa1, and the highly similar (86 % identity) peroxiredoxin, Tsa2, as well as a Prx5-type typical 2-Cys peroxiredoxin, Ahp1, a nuclear-localized atypical 2-Cys peroxiredoxin, Dot5, and a mitochondrial matrix-localized Prx6-type 1-Cys peroxiredoxin, Prx1. Yeast also contains three glutathione peroxidase-like proteins, Gpx1, Gpx2 and Gpx3, which have active-site cysteine residues instead of selenocysteine and are predominantly reduced by thioredoxins [47]. In addition, yeast contains two catalases, Ctt1 and Cta1, localized predominantly to the cytosol and peroxisomes respectively, as well as a mitochondrial intermembrane space-localized cytochrome *c* peroxidase, Ccp1 (Fig. 1a). We monitored Su9-roGFP2-Tsa2ΔC$_R$ responses to exogenous H_2O_2 or *t*-BuOOH at initial concentrations ranging from 0 to 2 mM in wild-type cells as well as cells individually deleted for the genes encoding both catalases, cytochrome *c* peroxidase, or each of the yeast thiol peroxidases (including Gpx1, Gpx2 and Gpx3 as well as four of the five peroxiredoxins; we omitted mitochondrial Prx1 as this was analyzed recently [34]). The response of the Su9-roGFP2-Tsa2ΔC$_R$ probe was followed in a fluorescence plate-reader as described previously [48]. For every probe response, we determined the integrated area under the background-corrected response curve between 0 and 2000 s (Fig. 1b). Intriguingly, our data revealed that deletion of *TSA1* led to a highly significant increase in Su9-roGFP2-Tsa2ΔC$_R$ probe response to both exogenous H_2O_2 and *t*-BuOOH, at concentrations from 20 to 200 and 20–40 μM respectively, compared to wild-type cells as well as all other gene deletion mutants ($P < 0.001$ for all samples) (Fig. 2a–f). Associated source data and full statistical analyses are available in an online data repository accessible at (https://doi.org/10.17632/62s536jngt.3). The additional deletion of the gene encoding Tsa2, to generate Δ*tsa1*Δ*tsa2* cells, made no significant difference to the Su9-roGFP2-Tsa2ΔC$_R$ probe response ($P = 0.999$ for Δ*tsa1* vs. Δ*tsa1*Δ*tsa2*) (Fig. 2a,d). At exogenous H_2O_2 and *t*-BuOOH concentrations above 500 μM and 100 μM respectively, no further increase in Su9-roGFP2-Tsa2ΔC$_R$ response was

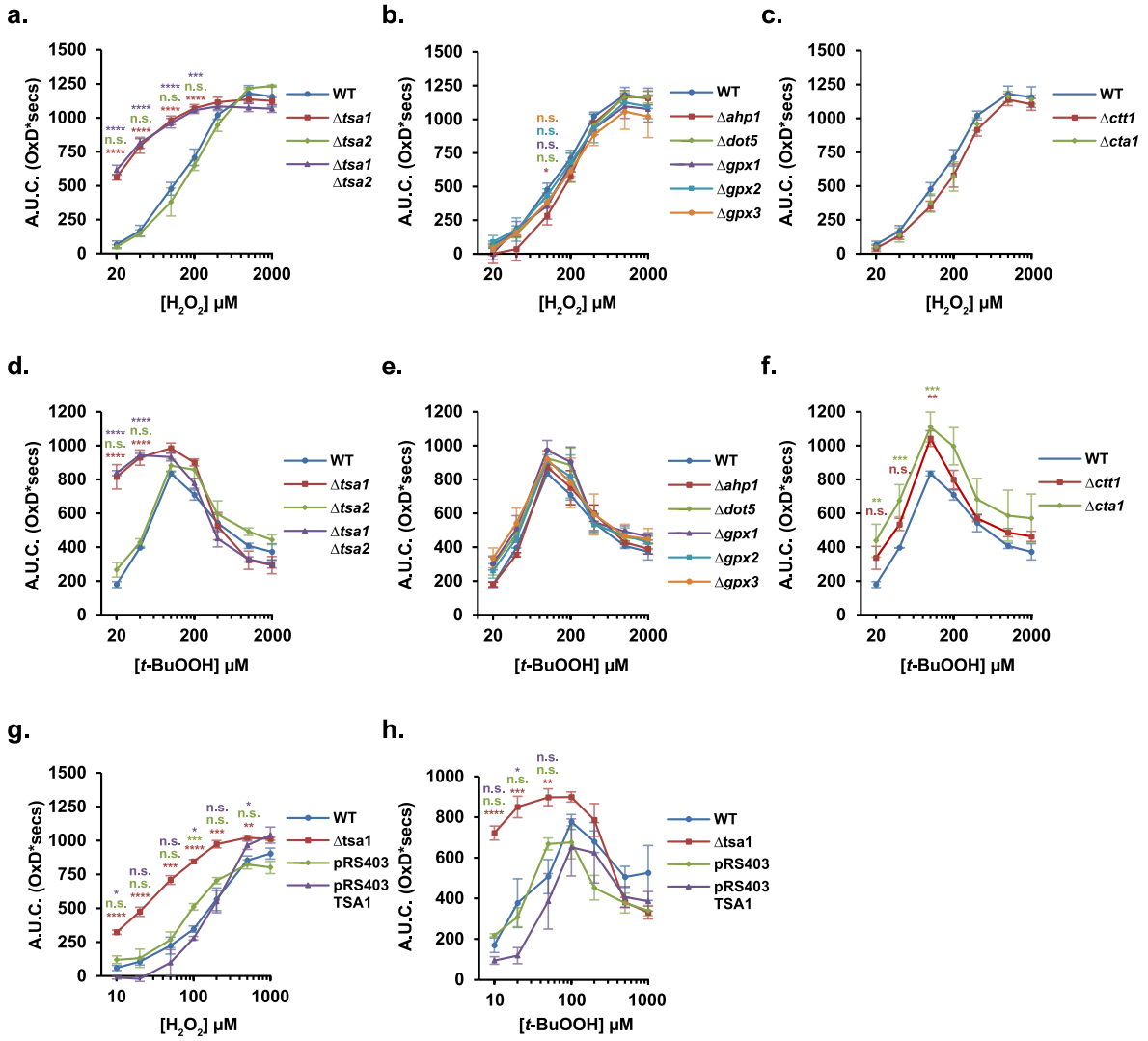

Fig. 2. Cellular peroxide scavenging is strongly dependent upon *TSA1* expression.
a,b,c. Su9-roGFP2-Tsa2ΔC$_R$ probe responses were measured in the indicated yeast deletion strains in response to exogenous H_2O_2 in the yeast strains indicated. The data for wild-type (WT) cells are replicated in each panel. **d,e,f.** Su9-roGFP2-Tsa2ΔC$_R$ probe responses were measured in the indicated yeast deletion strains in response to exogenous *t*-BuOOH in the yeast strains indicated. The data for WT are replicated in each panel. **g,h.** Su9-roGFP2-Tsa2ΔC$_R$ probe responses were measured in response to **g.** exogenous H_2O_2 or **h.** exogenous *t*-BuOOH applied to BY4742 wild-type or Δ*tsa1* cells, as well as BY4742 cells containing an empty genomically integrated pRS403 vector or a pRS403-*TSA1* vector, which provides cells with an additional copy of *TSA1*. Error bars in all panels represent the standard deviation for at least three independent repeats. P values were determined by a one-way ANOVA analysis followed by a Tukey's (HSD) test. P values for the difference between the WT and every other strain is represented on each panel with stars. The color of the stars corresponds to the respective deletion strain being compared to WT. n.s. = not significant, * = $P \leq 0.05$, ** = $P \leq 0.005$, *** = $P \leq 0.001$, **** = $P \leq 0.0001$.

observed for any strain as probe oxidation reached a maximum (Fig. 2a–f). Notably, at *t*-BuOOH concentrations greater than 100 μM, Su9-roGFP2-Tsa2ΔC$_R$ responses decreased in all strains compared to the response observed in 100 μM t-BuOOH treated cells (Fig. 2d–f). This effect is consistent with hyperoxidation and therefore inactivation of the Tsa2 moiety of the Su9-roGFP2-Tsa2ΔC$_R$ probe as we have shown previously [34,44,49,50]. In summary, our data suggest that Tsa1 alone is the major cytosolic peroxide scavenger and strongly limits the diffusion of both H_2O_2 and *t*-BuOOH through the yeast cytosol.

To further investigate our observations of the dominant importance of Tsa1, we next asked about the impact of overexpressing *TSA1*. To this end, we made use of a strain containing an extra genomic copy of the *TSA1* locus (generated using the integrative plasmid pRS403-*TSA1*) [51]. We observed a trend of decreased mitochondrial Su9-roGFP2-Tsa2ΔC$_R$ probe response in pRS403-*TSA1* cells, compared to wild-type and pRS403-empty controls, for both H_2O_2 and *t*-BuOOH at exogenous concentrations below 200 μM and 100 μM respectively (Fig. 2g and h), which was significant for some but not all concentrations of exogenous peroxide ($P < 0.05$). Thus, additional Tsa1 can further improve cytosolic peroxide removal.

Although Tsa1 was originally identified and purified as the dominant scavenger of peroxides in yeast [52] in accordance with our non-invasive intracellular measurements, it was surprising to us that we detected almost no effect of deleting the genes encoding any other thiol peroxidase or catalase. We thus asked if compensatory upregulation, perhaps including upregulation of Tsa1, may mask the effect of deleting other thiol peroxidases. To address this possibility, we investigated whether additional deletion of the peroxiredoxin genes *TSA2*, *AHP1* or *DOT5* in a Δ*tsa1* background would further impair H_2O_2 or *t*-BuOOH scavenging. Comparing Δ*tsa1* cells with Δ*tsa1*Δ*tsa2*, Δ*tsa1*Δ*ahp1*, Δ*tsa1*Δ*dot5*, Δ*tsa1*Δ*tsa2*Δ*ahp1* and Δ*tsa1*Δ*tsa2*Δ*dot5* cells, we observed no significant difference in the Su9-roGFP2-Tsa2ΔC$_R$ probe response at any concentration of H_2O_2 or *t*-BuOOH tested (Fig. 3a and b). For *t*-BuOOH-treated cells, in the Δ*tsa1* background, we observed an almost maximal mitochondrial Su9-roGFP2-Tsa2ΔC$_R$ probe response even at the lowest *t*-BuOOH concentration tested, i.e. 10 μM. Therefore, we repeated the experiment with exogenous *t*-BuOOH concentrations from 0.1 to 10 μM (Fig. S1a). This experiment also revealed no significant difference between Δ*tsa1* cells and Δ*tsa1*Δ*tsa2*, Δ*tsa1*Δ*ahp1*, Δ*tsa1*Δ*dot5*, Δ*tsa1*Δ*tsa2*Δ*ahp1* or Δ*tsa1*Δ*tsa2*Δ*dot5* cells at any *t*-BuOOH concentration tested, except for Δ*tsa1* vs. Δ*tsa1*Δ*ahp1* at 10 μM ($P = 0.03$). In summary, deletion of *TSA1* alone significantly impairs

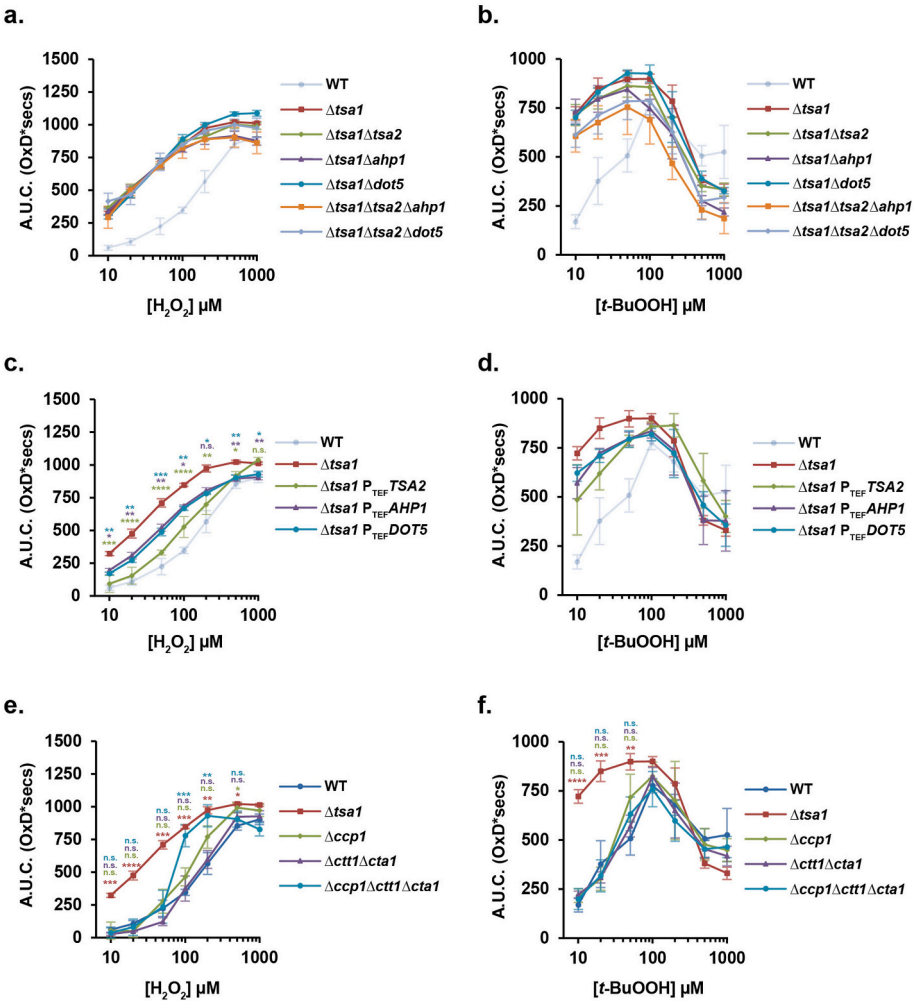

Fig. 3. Additional deletion of *TSA2*, *AHP1* or *DOT5* in a Δ*tsa1* background does not further decrease cellular peroxide scavenging.
a–f. Su9-roGFP2-Tsa2ΔC$_R$ probe responses were measured in the indicated yeast deletion and overexpression strains, in response to **a,c,e.** exogenous H_2O_2 or **b,d,f.** exogenous *t*-BuOOH applied at the indicated concentrations. The WT and Δ*tsa1* data for H_2O_2 treatment are replicated in Figs. 2g and 3a,c,e. The WT and Δ*tsa1* data for *t*-BuOOH treatment are replicated in Figs. 2h and 3b,d,f. Error bars in all panels represent the standard deviation for at least three independent repeats. P values were determined by a one-way ANOVA analysis followed by a Tukey's (HSD) test. P values for the difference between the Δ*tsa1* and every other strain (**a**–**d**) or between WT and every other strain (**e,f**) is represented on each panel with stars. The color of the stars corresponds to the respective deletion strain being compared to WT. n.s. = not significant, * = $P \leq 0.05$, ** = $P \leq 0.005$, *** = $P \leq 0.001$, **** = $P \leq 0.0001$.

cytosolic peroxide scavenging and further removal of other cytosolic peroxiredoxins does not exacerbate this phenotype.

Finally, we asked whether the overexpression of the genes encoding other cytosolic peroxiredoxins could improve cytosolic peroxide scavenging in a Δ*tsa1* background. To this end, we replaced the endogenous promoters of *TSA2*, *AHP1* or *DOT5* with a strong, constitutive TEF promoter in their genomic loci [53] to generate Δ*tsa1*P_{TEF}*TSA2*, Δ*tsa1*P_{TEF}*AHP1* and Δ*tsa1*P_{TEF}*DOT5* strains. We again monitored mitochondrial Su9-roGFP2-Tsa2ΔC$_R$ probe responses to exogenous H_2O_2 or *t*-BuOOH at concentrations from 0 to 1 mM. Interestingly, we observed a significant decrease in Su9-roGFP2-Tsa2ΔC$_R$ probe response in Δ*tsa1* P_{TEF}*TSA2*, Δ*tsa1* P_{TEF}*AHP1* and Δ*tsa1* P_{TEF}*DOT5* cells compared to Δ*tsa1* cells at all H_2O_2 concentrations from 0 to 200 μM (Fig. 3c). In response to *t*-BuOOH we observed a trend towards decreased Su9-roGFP2-Tsa2ΔC$_R$ responses in the Δ*tsa1*P_{TEF}*TSA2*, Δ*tsa1*P_{TEF}*AHP1* and Δ*tsa1*P_{TEF}*DOT5* strains compared to Δ*tsa1* at low *t*-BuOOH concentrations, however, these differences were not statistically significant ($P > 0.05$, Fig. 3d). At lower *t*-BuOOH concentrations, from 0.1 to 20 μM, we again observed a trend of decreased Su9-roGFP2-Tsa2ΔC$_R$ probe response in Δ*tsa1* P_{TEF}*TSA2*, Δ*tsa1*P_{TEF}*AHP1* and Δ*tsa1*P_{TEF}*DOT5* cells compared to Δ*tsa1* cells, but this was not significant at any concentration tested ($P > 0.05$, Fig. S1b). In summary, overexpression of *TSA2*, *AHP1* or *DOT5* increases cytosolic H_2O_2 scavenging in Δ*tsa1* cells but does not significantly increase *t*-BuOOH scavenging.

2.2. Cytochrome c peroxidase and catalases are collectively important at high H_2O_2 concentrations

In contrast to thiol peroxidases, which usually have micromolar K_m^{app} values, catalases use H_2O_2 as an oxidant *and* as a reductant, show no real substrate saturation, and do not require NADPH or a thiol adapter as electron donor during the regular catalytic cycle [54,55]. Therefore, it is thought that catalases are more important for scavenging at higher concentrations of H_2O_2, i.e., when thiol peroxidases are apparently saturated or inactivated by hyperoxidation, or when the NADPH-dependent replenishment of thiol pools might become rate-limiting [7,56]. The two catalases in yeast are also much less abundant than Tsa1 [12]. Indeed, as shown in Fig. 2, individual deletion of either *CTA1* or *CTT1*, had no significant impact on scavenging at any H_2O_2 concentration tested. Importantly, catalases are unable to catalyze *t*-BuOOH reduction, which thus serves as a negative control for further experiments. We therefore asked whether deletion of *CTA1* and *CTT1* in combination would have an impact on cytosolic H_2O_2 scavenging. Furthermore, we investigated the relevance of the mitochondrial intermembrane space-localized cytochrome *c* peroxidase, Ccp1. We observed no difference in mitochondrial Su9-roGFP2-Tsa2ΔC$_R$ probe response between wild-type cells and Δ*ccp1*, Δ*ctt1*Δ*cta1*, or Δ*ccp1*Δ*ctt1*Δ*cta1* cells at H_2O_2 concentrations from 10 to 50 μM (Fig. 3e). However, at higher H_2O_2 concentrations, i.e. 100 and 200 μM, we observed a significant increase in Su9-roGFP2-Tsa2ΔC$_R$ probe response in Δ*ccp1*Δ*ctt1*Δ*cta1* cells compared to wild-type cells ($P < 0.005$). The Su9-roGFP2-Tsa2ΔC$_R$ probe response at this concentration was similarly increased as in Δ*tsa1* cells. These observations thus suggest that Ccp1, Cta1 and Ctt1 in combination have a similar impact on scavenging of higher concentrations of H_2O_2 as Tsa1 but that, even in combination, they are not relevant at lower H_2O_2 concentrations. In contrast, we observed no significant difference in the response of the Su9-roGFP2-Tsa2ΔC$_R$ probe to *t*-BuOOH in any strain compared to wild-type cells, except for the Δ*tsa1* control (Fig. 3f). Thus, our results indicate that catalases and cytochrome *c* peroxidase are only important in combination for removal of higher concentrations of H_2O_2, which seems consistent with the kinetic parameters and substrate specificity of catalases and cytochrome *c* peroxidase.

2.3. HyPer7 responds specifically to H_2O_2 but poorly to t-BuOOH

Thus far, all our measurements were performed in cells grown with a non-fermentable glycerol/ethanol mix as the carbon source. However, yeast cells grown on high glucose are known to repress mitochondrial biogenesis as well as repress the general stress response pathway [57–59]. We were thus interested to see if our observations were reproducible in cells grown on glucose as the sole carbon source, particularly when cells were harvested at a low cell density, i.e. when the glucose concentration in the medium is still high. Our Su9-roGFP2-Tsa2ΔC$_R$-based assay is not compatible with cells grown in glucose as, due to repression of mitochondrial biogenesis, the matrix-localized Su9-roGFP2-Tsa2ΔC$_R$ fluorescence is too low for reliable measurements. We therefore turned to an alternative assay, namely expressing genetically encoded H_2O_2 probes in the cytosol to study the ability of endogenous H_2O_2 scavenging enzymes to compete with the probe for H_2O_2. We chose not to use roGFP2-Tsa2ΔC$_R$ for these studies as we have previously shown that this probe forms heterooligomers with endogenous Tsa1 [44]. We wanted to avoid any possibility for our results to be confounded by possible differences in probe behavior dependent upon whether it could co-assemble with endogenous Tsa1 or not. Instead, we turned to the ultrasensitive H_2O_2 probe HyPer7 [45]. Preliminary characterization revealed that HyPer7, expressed in wild-type cells, responds less sensitively to exogenous H_2O_2 than roGFP2-Tsa2ΔC$_R$ (Figs. S2a and c). Whilst cytosolic roGFP2-Tsa2ΔC$_R$ responds to as little as 10 μM exogenous H_2O_2, HyPer7 showed no response until exogenous H_2O_2 was applied at a concentration of 50 μM or higher. Interestingly, we observed that HyPer7 was barely responsive to *t*-BuOOH, which is consistent with previous *in vitro* data [45], whereas roGFP2-Tsa2ΔC$_R$ responded to *t*-BuOOH at a concentration of 10 μM or above (Figs. S2b and d). Thus, for all further experiments we limited ourselves to monitoring the response to H_2O_2 alone. HyPer7 containing a mutation of the reactive cysteine, HyPer7 C121S, was completely unresponsive to either H_2O_2 or *t*-BuOOH at any concentration tested and served as a negative control (Figs. S2e and f). Furthermore, we investigated the relative importance of the cytosolic thioredoxin and glutaredoxin systems for HyPer7 reduction. We observed that both the steady-state HyPer7 fluorescence excitation ratio, as well as the response to exogenous H_2O_2 was strongly increased in Δ*trx1*Δ*trx2* cells in comparison to wild-type cells, whilst we observed no difference between wild-type and Δ*grx1*Δ*grx2* cells (Figs. S3a–d). We thus conclude that HyPer7 is predominantly reduced by cytosolic thioredoxins, confirming previous reports [60,61], and in contrast to the GSH/glutaredoxin-dependent reduction of roGFP2-Tsa2ΔC$_R$ [44].

2.4. Tsa1 scavenges the majority of H_2O_2 in the cytosol of cells grown with glucose as carbon source

Satisfied that HyPer7 specifically responds to H_2O_2 in our yeast system, we next turned to using it to address the relative importance of the various H_2O_2 scavengers in glucose-grown cells. Consistent with our Su9-roGFP2-Tsa2ΔC$_R$ data, we show that cytosolic HyPer7 is much more efficiently oxidized by H_2O_2 in Δ*tsa1* cells as compared to wild-type cells (Fig. 4a). The HyPer7 response was not significantly increased in any other thiol peroxidase deletion mutant when compared to wild-type cells at any H_2O_2 concentration tested (Fig. 4a and b). Intriguingly, in the Δ*tsa1* cells, the sensitivity of the HyPer7 response to H_2O_2 is comparable to that of roGFP2-Tsa2ΔC$_R$, with HyPer7 responding to as little as 10 μM exogenous H_2O_2 (compare Figs. 2a and 4a). We interpret this to mean that endogenous Tsa1, due to its high concentration and high H_2O_2 reactivity, efficiently outcompetes HyPer7 for H_2O_2. In the absence of Tsa1, HyPer7 becomes the most abundant and efficient H_2O_2 scavenger in the cell and can then effectively compete for H_2O_2. Finally, we monitored the HyPer7 response to H_2O_2 in Δ*ccp1*, Δ*cta1*, Δ*ctt1* and Δ*ccp1*Δ*ctt1*Δ*cta1* cells in comparison to wild-type cells. Consistent with

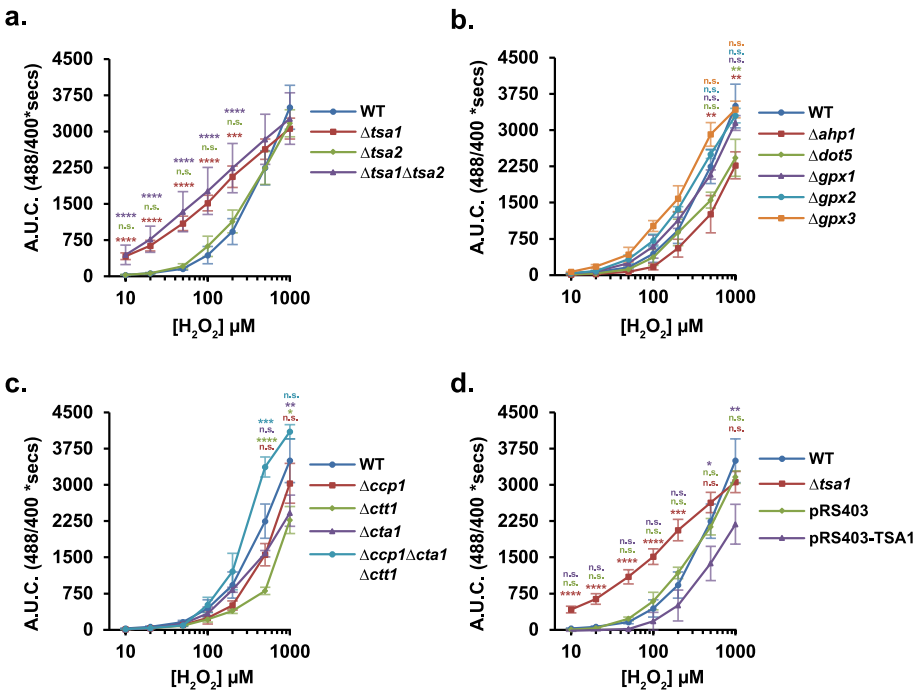

Fig. 4. Cytosolic HyPer7 enables measurements of the cellular peroxide scavenging capacity in glucose containing media.
a–d. HyPer7 responses were measured in the indicated yeast deletion strains in response to exogenous H_2O_2 applied at the indicated concentrations. The integrated A.U.C. was calculated for the first 2000 s of the probe response. The data for wild-type (WT) cells are replicated in each panel. The data for Δ*tsa1* cells is replicated in panels **a**. and **d**. Error bars in both panels represent the standard deviation for at least three independent repeats. P values were determined by a one-way ANOVA analysis followed by a Tukey's (HSD) test. P values for the difference between the WT and every other strain is represented on each panel with stars. The color of the stars corresponds to the respective deletion strain being compared to WT. n.s. = not significant, * = $P \leq 0.05$, ** = $P \leq 0.005$, *** = $P \leq 0.001$, **** = $P \leq 0.0001$.

our Su9-roGFP2-Tsa2ΔC$_R$ results, we observed no significant impact of catalase or cytochrome *c* peroxidase deletion on HyPer7 response at lower concentrations of exogenous H_2O_2 (Fig. 4c). However, we did observe a significant increase in HyPer7 response in Δ*ccp1*Δ*ctt1*Δ*cta1* cells in comparison to wild-type cells at 500 µM exogenous H_2O_2 ($P = 0.0005$). An additional *TSA1* locus decreased the HyPer7 response comparable to the roGFP2-Tsa2ΔC$_R$ response in Fig. 2g (Fig. 4d). Similar effects as observed for all deletion strains in Fig. 4a–d were also seen in cells grown on non-fermentable glycerol/ethanol medium (Fig. S4). In summary, our observations of HyPer7 responses in the cytosol of glucose and glycerol/ethanol-grown cells support the conclusion that Tsa1 is the dominant scavenger of H_2O_2 under both fermentative and respiratory conditions. Catalases and cytochrome *c* peroxidase only have a significant impact on cellular H_2O_2 scavenging capacity when deleted in combination and even then, are only important at higher H_2O_2 concentrations.

2.5. *TSA1 deletion induces compensatory upregulation of pentose phosphate pathway enzymes*

We next sought to understand whether TSA1 deletion resulted in proteome rewiring. To this end, we performed label-free quantitative proteome analysis of wild-type and Δ*tsa1*Δ*tsa2* cells. We observed large proteomic changes, with 193 and 145 proteins being significantly more or less abundant respectively, in the Δ*tsa1*Δ*tsa2* strain (Fig. S5). GO term overrepresentation analysis for up-regulated proteins indicated changes in carbohydrate metabolism in response to reactive oxygen species. In particular, glucose-6-phosphate metabolism, which is required to fuel the pentose phosphate pathway (PPP) – the most important source of cytosolic NADPH — was among the most significant terms and several PPP enzymes were among the most strongly up-regulated proteins (Fig. S5). Interestingly, we saw no enrichment for proteins whose corresponding genes are under the regulation of Yap1, which is consistent with a previous report of no change in Yap1-dependent transcription in a Δ*tsa1* background [62]. No significantly enriched terms were detected for down-regulated proteins.

2.6. *Tsa1 is a major source of cellular glutathione peroxidase activity*

The addition of H_2O_2 to budding yeast leads to the production of cellular GSSG, which is particularly evident in cells deleted for *GLR1*, which encodes glutathione reductase [63]. However, the enzyme(s) responsible for the glutathione peroxidase-like activity in yeast remain unclear. Yeast has three proteins, Gpx1, Gpx2 and Gpx3, that are structurally related to mammalian glutathione peroxidases [22,24,26]. Although glutathione-dependent activities were reported for the yeast glutathione peroxidase isoforms [22,24,26], no rate constants were determined, and Gpx3 was shown to be much more active with reduced thioredoxins than GSH [47], which is in accordance with GSH-dependent mammalian glutathione peroxidases being rather the exception [64]. We recently demonstrated that the peroxiredoxin Prx1 is an important source of GSSG in the mitochondrial matrix upon H_2O_2 treatment although the impact upon total cellular GSSG levels is minor [34]. Given the dominant role of Tsa1 in H_2O_2 reduction, coupled with the recent observation that GSH can serve as an electron donor for the reduction of human PRDX2 [65], we asked whether Tsa1 is involved in H_2O_2-dependent GSSG production.

To address this question, we used a roGFP2-Grx1 probe [66] to monitor the response of the cytosolic glutathione steady-state redox potential to exogenous H_2O_2 addition. We performed these experiments in cells deleted for *GLR1*, the gene encoding glutathione reductase, to sensitize the glutathione pool to oxidation. In this background we additionally deleted *TSA1* and/or *TSA2* to generate Δ*glr1*, Δ*glr1*Δ*tsa1*, *glr1*Δ*tsa2* and Δ*glr1*Δ*tsa1*Δ*tsa2* cells. Intriguingly, we observed a strong and significantly decreased probe response in both Δ*glr1*Δ*tsa1* and Δ*glr1*Δ*tsa1*Δ*tsa2* cells compared to Δ*glr1*, indicating less GSSG formation, despite the much less efficient H_2O_2 scavenging in the absence of Tsa1 (Fig. 5). We observed no significant difference in glutathione probe

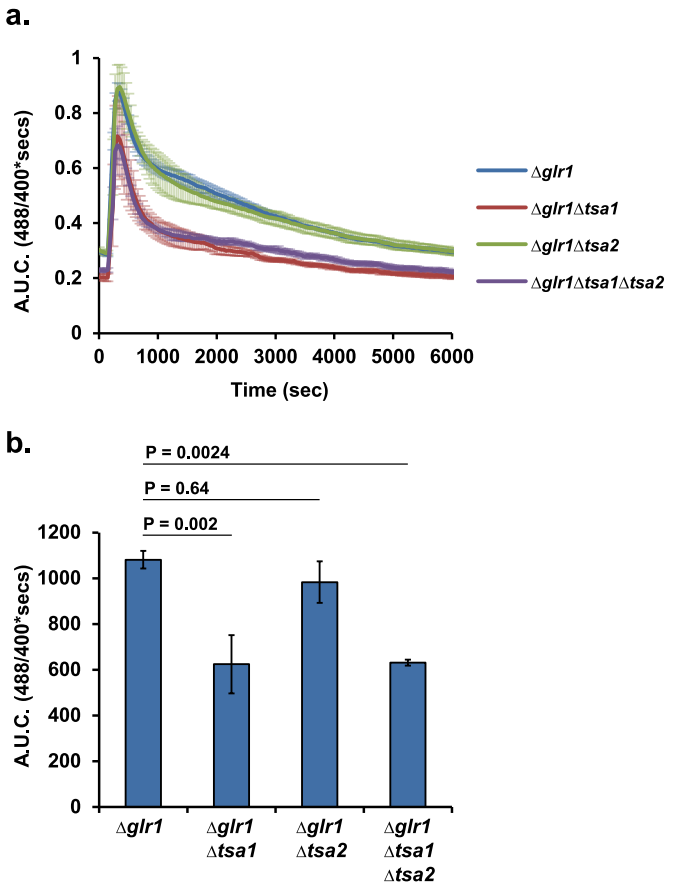

Fig. 5. Tsa1 is a major source for cytosolic GSSG.
a. Cytosolic roGFP2-Grx1 responses measured in BY4742 wild-type, Δ*glr1*, Δ*glr1*Δ*tsa1*, Δ*glr1*Δ*tsa2* and Δ*glr1*Δ*tsa1*Δ*tsa2* cells in response to the addition of 1 mM H_2O_2 at the indicated time-point. **b.** A.U.C. of the roGFP2-Grx1 responses shown in panel **a.** for the first 6000 s. Error bars in all panels represent the standard deviation for at least three independent repeats. P values were determined by a one-way ANOVA analysis followed by a Tukey's (HSD) test.

response between Δ*glr1* and Δ*glr1*Δ*tsa2* cells (Fig. 5). To exclude that the results are a *GLR1* deletion-dependent phenotype, we also monitored the responses of Grx1-roGFP2 [66] and roGFP2-Tsa2ΔC$_R$ probes in wild-type and Δ*tsa1*Δ*tsa2* cells to monitor the response of the cytosolic glutathione steady-state redox potential and H_2O_2 level to exogenous H_2O_2 addition (Fig. S6). Consistent with the data in Fig. 5, we saw a strongly decreased Grx1-roGFP2 response and an increased roGFP2-Tsa2ΔC$_R$ response in Δ*tsa1*Δ*tsa2* cells compared to wild-type cells. Our results indicate that Tsa1 can use GSH as either a direct or indirect reductant. Thus, under the chosen assay conditions, Tsa1 is an important source of H_2O_2-dependent GSSG production.

2.7. GSH slowly reduces Tsa1 in vitro

To assess whether cytosolic thioredoxins, glutaredoxins and/or GSH are efficient direct reductants of Tsa1, we determined the according rate constants in stopped-flow kinetic measurements (Figs. 6–8). To confirm our experimental setup, we mixed reduced Tsa1 in the first syringe with H_2O_2 in the second syringe revealing two or three distinct kinetic phases based on the altered tryptophan fluorescence of the enzyme as reported previously for Prx1-type typical 2 Cys peroxiredoxins [67–70] (Fig. 6a and b). A rapid decrease in fluorescence during the first phase depended on the H_2O_2 concentration and usually occurred during the dead-time of the measurement at higher H_2O_2 concentrations (Fig. 6b). This reaction phase reflects the sulfenic acid formation of the peroxidatic cysteinyl residue (Fig. 6a). The increase in fluorescence during the second phase and decrease in fluorescence during the third phase did not depend on the H_2O_2 concentration (Fig. 6b). These phases can be assigned to local protein unfolding and intersubunit disulfide bond formation between the peroxidatic and resolving cysteinyl residue [68–70]. The separation of the local unfolding and disulfide bond formation into two kinetic phases usually does not occur in mammalian Prx1-type enzymes but has been previously reported for Tsa1 and PfPrx1a from *Plasmodium falciparum* [68,69]. Furthermore, hyperoxidation of Tsa1 should be less than 1 % under the chosen assay conditions [68], and we therefore omitted this side reaction in our assignment and reaction scheme (Fig. 6a). A slow fourth and a very slow fifth phase were only detected when GSH was added to reduced Tsa1 in the first syringe (Fig. 6c and d). The observed rate constant (k_{obs}) for the increase in fluorescence during the fourth phase depended on the GSH concentration. A rather small second order rate constant k_{GSH} of 2.9 $M^{-1}s^{-1}$ and a GSH-independent

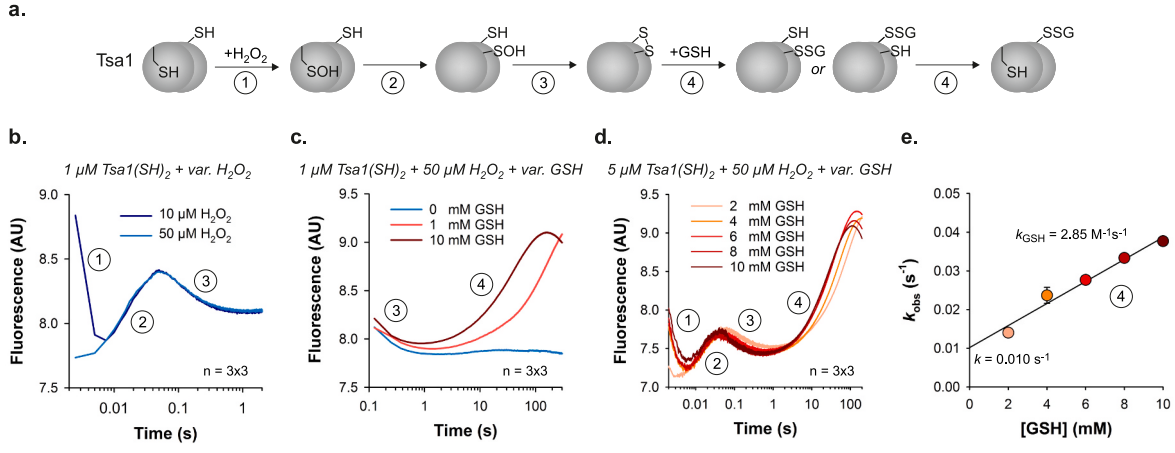

Fig. 6. Nonenzymatic reduction of oxidized Tsa1 by GSH.
a. Reaction scheme for the oxidation of reduced Tsa1 by H_2O_2 (step 1), local unfolding (step 2), intramolecular disulfide bond formation (step 3), nonenzymatic glutathionylation and subsequent local refolding of Tsa1 (step 4). **b.** Stopped-flow kinetic measurement of the Tsa1 tryptophan fluorescence for the oxidation of reduced recombinant Tsa1 by H_2O_2 at 25 °C and pH 7.4. Reaction steps 1–3 were assigned according to the scheme in panel a. The kinetic traces represent averages from technical triplicate measurements. **c,d.** Stopped-flow kinetic measurements as in panel b. with either 1 or 5 μM reduced Tsa1 and variable concentrations of GSH in the first syringe and H_2O_2 in the second syringe revealed a GSH-dependent fourth phase. **e.** Secondary plot of the k_{obs} values (derived from single exponential fits of the fourth phase) against the GSH concentration from panel d. Error bars in panel e represent the standard deviation for three independent biological replicates.

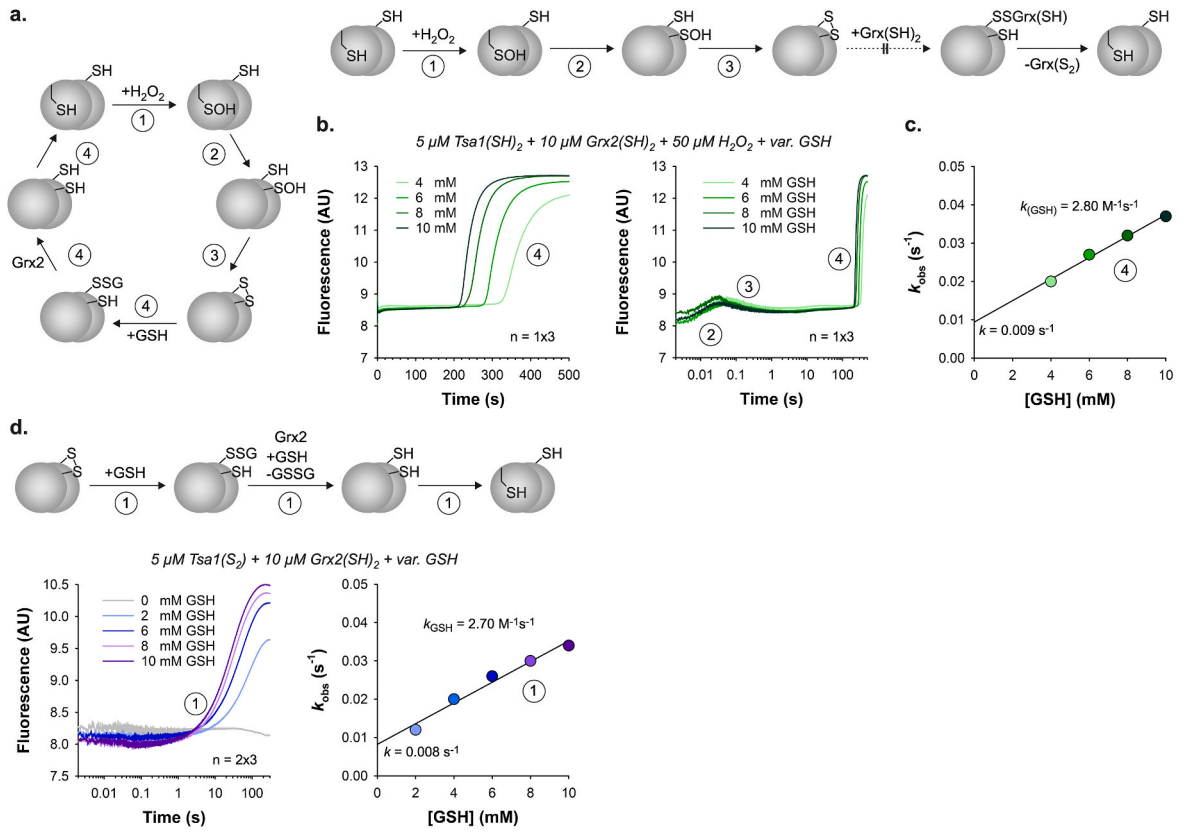

Fig. 7. Grx2 reacts with glutathionylated Tsa1 but not with Tsa1(S_2).
a. Reaction schemes for the reduction of glutathionylated Tsa1 (left side) or of Tsa1(S_2) (right side) by reduced Grx2. **b.** Stopped-flow kinetic measurement of the Tsa1 tryptophan fluorescence for the oxidation of reduced recombinant Tsa1 by H_2O_2 in the presence of Grx2 and variable concentrations of GSH at 25°C and pH 7.4. All reduced compounds were in the first syringe and H_2O_2 was in the second syringe. Reaction steps 1-4 were assigned according to the schemes in panel a. **c.** Secondary plot of the k_{obs} values (derived from single exponential fits of the fourth phase) against the GSH concentration from panel b. **d.** Reaction scheme, stopped-flow kinetic measurement and secondary plot for the reaction between Tsa1(S_2) in the first syringe and reduced Grx2 and variable concentrations of GSH in the second syringe. The kinetic traces in panels b and d represent averages from technical triplicate measurements. Values in the secondary plots in panels c and d were from single or double biological replicates.

rate constant of 0.010 s^{-1} were determined from the slope and y-axis intercept of a secondary plot (Fig. 6e). We assigned k_{GSH} to the nonenzymatic reduction of the intersubunit disulfide bond by GSH, whereas the GSH-independent rate constant might reflect a conformational change, the reverse reaction or a transfer of the glutathione moiety between the peroxidatic and resolving cysteinyl residue. Alternatively, the data from the secondary plot could be hyperbolically fitted through the origin, resulting in a slightly higher apparent k_{GSH} value of $\leq$8 $M^{-1}s^{-1}$, as estimated from the tangent at low GSH concentrations. The strong increase in fluorescence towards the potential initial fluorescence of the experiment suggests that the local refolding of Tsa1 (which necessitates a reduced and not a glutathionylated peroxidatic cysteinyl residue) also occurs during the fourth phase (Fig. 6c and d). However, this step is kinetically masked by the rate-limiting nonenzymatic reduction of the intersubunit disulfide bond (Fig. 6a).

2.8. Glutaredoxin does not catalyze the glutathionylation of Tsa1 in vitro

Next, we analyzed whether the addition of reduced recombinant Grx2 affects the catalytic cycle and the reaction kinetics (Fig. 7a). Recombinant Grx2, which shares 64 % sequence identity with Grx1, was chosen because it accounts for 80 % of the physiological glutaredoxin activity in yeast cell extracts and protects yeast against the treatment with H_2O_2, $FeCl_3$, menadione or paraquat [71,72]. Considering a potential glutaredoxin-dependent reduction of the Tsa1 disulfide, Tsa1(S_2), Grx2 might either directly reduce Tsa1 following a dithiol:disulfide exchange mechanism or activate GSH for protein disulfide reduction [64,73–75]. Although the chosen Grx2 concentration was at least four times higher than the estimated cytosolic concentration of Grx2 [7], no additional phases were observed with 10 µM reduced Grx2, indicating that Tsa1(S_2) does not react directly with Grx2 under the chosen assay conditions (Fig. 7b). In contrast to the reaction with GSH in the absence of Grx2 (Fig. 6), we detected a lag phase between the third and fourth phase when reduced Grx2 and GSH were both added to reduced Tsa1 in the first syringe (Fig. 7b). We interpret the lag phase as a cyclic Grx2-catalyzed deglutathionylation and H_2O_2-dependent oxidation of Tsa1 that results in the consumption of H_2O_2. These steps are masked during the lag phase because they are much faster than the nonenzymatic glutathionylation of Tsa1. The rate-limiting nonenzymatic glutathionylation and local refolding of Tsa1 only became detectable at the end of the last catalytic cycle. This interpretation is supported by the almost identical GSH-dependent second order rate constant as for the fourth phase without Grx2 (Figs. 6d and 7c). Based on the rate constant and the used concentrations, we estimated that about 20–30 µM H_2O_2 were consumed during the 200–330 s lag phase. The difference to the 50 µM H_2O_2 used in the assay could be explained by a slightly higher rate constant (e.g., from hyperbolic fits of the secondary plots as outlined above) or the additional nonenzymatic reduction of H_2O_2 by Grx2 and/or GSH [76]. Stopped-flow experiments with Tsa1(S_2) in the first syringe and reduced Grx2 and GSH in the second syringe revealed a single-phase increase of fluorescence in accordance with the fourth phase from Fig. 6c and d, again confirming a rate-limiting nonenzymatic reaction with a rate

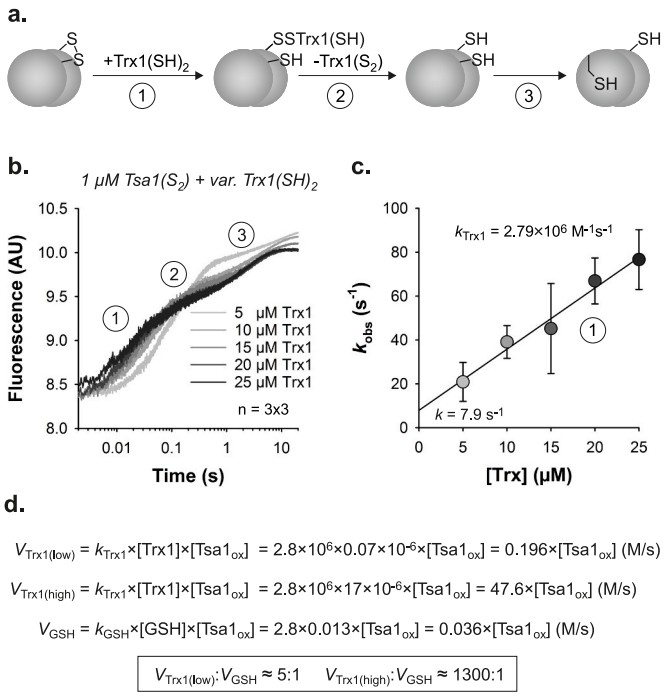

Fig. 8. Trx1 rapidly reduces Tsa1(S_2).
a. Reaction scheme for the reduction of Tsa1(S_2) by reduced Trx1. **b.** Stopped-flow kinetic measurement of the Tsa1 tryptophan fluorescence for the reduction of recombinant Tsa1(S_2) by reduced Trx1 at 25 °C and pH 7.4. Reaction steps 1–3 were (provisionally) assigned according to the scheme in panel a. The kinetic traces represent averages from technical triplicate measurements. **c.** Secondary plot of the k_{obs} values (derived from single exponential fits of the first phase) against the Trx1 concentration from panel b. Error bars in panel c represent the standard deviation for three independent biological replicates. **d.** Kinetic comparison of the reductions rates for Tsa1(S_2) by Trx1 or GSH based on estimates for the physiological concentration of the reaction partners.

constant k_{GSH} of 2.7 $M^{-1}s^{-1}$ despite the presence of Grx2 (Fig. 7d). In summary, Grx2 is neither a direct reductant for Tsa1(S_2) nor activates GSH for Tsa1 reduction, and the rapid Grx2-catalyzed deglutathionylation of Tsa1 is kinetically masked by the rate-limiting nonenzymatic reaction between Tsa1(S_2) and GSH.

2.9. Nonenzymatic reduction of Tsa1 by GSH would require oxidation of the thioredoxin pool

Recombinant Trx1 was previously shown to reduce Tsa1 in steady-state kinetic assays [67]. We now determined the rate constants for the Trx1-dependent reduction of Tsa1 using stopped-flow measurements with Tsa1(S_2) in the first syringe and variable concentrations of reduced Trx1 in the second syringe (Fig. 8a and b). The detected increase in fluorescence could be subdivided into three phases (Fig. 8b). The k_{obs} values for the strong increase in fluorescence during the first phase depended on the Trx1 concentration (Fig. 8c). A second order rate constant k_{Trx1} of 2.8 × 10^6 $M^{-1}s^{-1}$ and a Trx1-independent rate constant of 7.9 s^{-1} were determined from the slope and y-axis intercept of the secondary plot (Fig. 8c). We assign k_{Trx1} to the reduction of Tsa1(S_2) yielding a mixed disulfide with Trx1 (whereas the Trx1-independent rate constant might reflect a conformational change or the reverse reaction). The second and third phase appeared to be independent of the Trx1 concentration and remain to be analyzed in more detail. We provisionally assign these two phases to the formation of the Trx1 disulfide, Trx1(S_2), and the subsequent local refolding of reduced Tsa1 (Fig. 8a and b). Taking into account calculated estimates for the cytosolic concentration of Trx1 between 0.07 and 17 μM [7] and GSH around 13 mM [77], we then compared the reduction rates for Tsa1 (S_2) (Fig. 8d). At an estimated low Trx1 concentration of 0.07 μM, the reduction of Tsa1 by Trx1 would be about five times faster than by GSH and 20 % of Tsa1 might be reduced by GSH. However, this calculation neglects the presence of Trx2, which shares 78 % sequence identity with Trx1, has a similar abundance, and also efficiently reacts with Tsa1 [67]. At an estimated high Trx1 concentration of 17 μM, the reduction of Tsa1 by Trx1 would be about 1.3 × 10^3 times faster than by GSH and only 0.08 % of Tsa1 might be reduced by GSH (neglecting again the presence of Trx2) (Fig. 8d). To exclude that GSSG is formed by the nonenzymatic reduction of thioredoxins, we also performed control experiments with Trx1(S_2) and GSH, yielding an estimated second order rate constant <1 $M^{-1}s^{-1}$ (Fig. S7a). Adding either 10 μM Grx2($SH)_2$ or 0.4 U/ml glutathione reductase and NADPH did not accelerate the nonenzymatic GSH-dependent reduction of Trx1(S_2) (Figs. S7b and c). Thus, Grx2 does not activate GSH for the reduction of Trx1 and a direct reduction of Trx1 (S_2) by GSH is too slow to explain the observed Tsa1-dependent GSSG formation in yeast. In summary, provided that Trx1 and Trx2 are efficiently reduced by thioredoxin reductase, the thioredoxins are most likely the dominant physiological reductants for Tsa1. A nonenzymatic reduction of Tsa1 by GSH, followed by the rapid Grx2-dependent formation of GSSG, requires either a depletion or oxidation of the thioredoxin pool, which probably occurs at high bolus peroxide treatments [35,46].

3. Discussion

The efficiency of cellular H_2O_2 removal, and the identity of the proteins that facilitate it, has important implications for our understanding of both H_2O_2 toxicity and the mechanisms by which H_2O_2 functions as a signaling molecule [4,29,78–80]. Our observation that the diffusion of peroxide through the cell is strongly limited by Tsa1 is consistent with previous *in silico* studies, which suggested that peroxiredoxins in general should strongly limit H_2O_2 diffusion [81–83], studies of budding yeast growth dynamics and the adaptation to H_2O_2 challenge [84], and by recent observations in fission yeast and mammalian cells, which reported that peroxiredoxin- and thioredoxin reductase-dependent H_2O_2 scavengers control intracellular H_2O_2 diffusion [37,43,85–87]. Taken together, these observations show that steep intracellular H_2O_2 gradients do exist and that they are shaped by endogenous thiol peroxidase-dependent scavenging. It will be extremely interesting in the future to test whether intracellular H_2O_2 gradients have a role in H_2O_2 signaling, for example by helping to ensure specificity. It might be important, that only a specific fraction of a certain protein, in a defined subcellular localization, is oxidized by H_2O_2. This could be achieved by co-localization of a peroxiredoxin, target protein and H_2O_2 source in specific microdomains, which may be mediated by scaffold proteins [88,89], or by a local inactivation of a peroxiredoxin by posttranslational modifications [41].

We demonstrate unequivocally that Tsa1 is the dominant scavenger of both H_2O_2 and *t*-BuOOH, when applied exogenously at low micromolar concentrations to budding yeast cells. This observation holds true under both fermentative and respiratory conditions. Our findings reveal a similarity to the situation previously reported in *Escherichia coli*, where only the alkylhydroperoxide reductase AhpC is relevant for peroxide scavenging at low H_2O_2 concentrations [56,90,91]. *E. coli* harbor other proteins, that display thiol peroxidase activity *in vitro*, but their contribution to *in vivo* H_2O_2 detoxification appears negligible [90]. Nonetheless, the situation is more complex in budding yeast, as it is in most eukaryotes, with budding yeast harboring eight thiol peroxidases, two catalases and a cytochrome *c* peroxidase. Therefore, the bigger question is why cells harbor multiple thiol peroxidases when in many cases only one plays a major role in peroxide removal. The answer to this question remains unclear but may well lie in alternative functions, for example the participation of thiol peroxidases in redox relays, which facilitate the transfer of oxidative equivalents from H_2O_2 to specific target proteins to regulate function or activity [29,

38,47,79,80,92,93]. Another explanation could be different substrate preferences or degrees of substrate promiscuity, e.g. for lipid hydroperoxides as electron acceptors or alternative thiols as electron donors. Such properties are indeed reflected by the structural and mechanistic versatility of thiol peroxidases [3,64,69]. Alternatively, some proteins may be important for peroxide removal in specific subcellular compartments, affording protection in these domains, but having a negligible impact on the overall cellular H_2O_2 scavenging capacity.

We show that the two catalases and cytochrome *c* peroxidase in yeast only have a noticeable effect on cellular H_2O_2 scavenging capacity when deleted in combination, and even then, only at higher H_2O_2 concentrations. This is consistent with the known enzymatic properties of catalases and peroxiredoxins, i.e. catalases cannot be saturated by H_2O_2 and do not require a thiol reductant, which allows them to function at very high peroxide concentrations when thioredoxins are oxidized and/or peroxiredoxins are hyperoxidized [7,37,43].

In terms of H_2O_2 toxicity, surprisingly, we still do not fully understand the mechanisms by which H_2O_2 leads to cell death, especially in eukaryotes. In prokaryotes, this question has been extensively studied, for example in *E. coli*. The predominant mechanism of H_2O_2-induced cell death seems to be indirect damage to DNA via the iron-dependent production of hydroxyl radicals, as well as damage to iron-sulfur clusters [94,95]. However, in eukaryotes, H_2O_2-dependent oxidative damage does not seem sufficient to fully explain H_2O_2 toxicity, particularly when H_2O_2 is present at low micromolar to millimolar concentration. Instead, recent studies have pointed to the depletion of pools of reduced thioredoxin and reduced glutathione [34,35] as well as modulation of PKA activity as important mediators of H_2O_2-dependent cell death [96]. Tsa1 was suggested to repress PKA activity in the presence of H_2O_2. In a Δ*tsa1* strain, which originally displays a higher sensitivity to H_2O_2-dependent cell death than wild-type cells, wild-type-like H_2O_2 resilience could be gained by mutations that constitutively repress PKA activity [96]. Molin and co-workers concluded that whilst '*Tsa1 is required for both promoting resistance to H_2O_2 and extending lifespan upon caloric restriction … Tsa1 effects both these functions not by scavenging H_2O_2, but by repressing the nutrient signaling Ras-cAMP-PKA pathway at the level of the protein kinase A (PKA) enzyme*' [96]. This could thus support the conclusion that the sensitivity of Δ*tsa1* cells to H_2O_2 is independent of a loss of H_2O_2 scavenging. On the other hand, inactivation of PKA leads to expression of an array of stress resistance enzymes that may increase H_2O_2 scavenging capacity,. Decreased PKA repression and thus decreased stress resistance enzyme expression in the absence of Tsa1 might still provide a plausible link between cellular H_2O_2 scavenging capacity and cell death. Therefore, whether or not there is a direct link between H_2O_2 scavenging capacity and cell death still remains to be fully answered.

Finally, we showed that *in vitro* Tsa1 is efficiently reduced by yeast Trx1 but not by Grx2 and/or GSH, suggesting that the intracellular Tsa1-dependent GSSG production requires (i) a depletion or oxidation of the thioredoxin pool and (ii) the presence of a reduced glutaredoxin to reduce the mixed disulfide between glutathione and Tsa1. Alternatively, Tsa1 might transfer its oxidation to another protein than Trx1 that is efficiently reduced by the GSH/glutaredoxin system. The rate constant of $2.8 \times 10^6\ M^{-1}s^{-1}$ for the reduction of Tsa1(S_2) by yeast Trx1 is very similar to the rate constants for the reduction of the human Prx1-type typical 2 Cys peroxiredoxin PRDX1 by human Trx1 and Trx2 [70], the rate constant for the reduction of the Prx1-type typical 2 Cys peroxiredoxin c-TXNPx from *Trypanosoma cruzi* by tryparedoxin [97], the rate constant for the reduction of the human Prx5-type atypical 2 Cys peroxiredoxin PRDX5 by human Trx2 [98], and the rate constants for the reduction of the sulfenic acid of the promiscuous Prx5-type 1 Cys peroxiredoxin PfAOP from *Plasmodium falciparum* by GSH and other low-molecular-weight thiols [69,99]. In contrast, the million times smaller rate constant for the reduction of Tsa1(S_2) by GSH of $2.9\ M^{-1}s^{-1}$ indicates a rate-limiting nonenzymatic thiol:disulfide exchange reaction, which is followed by a rapid Grx2-dependent deglutathionylation and GSSG formation. An analogous reaction sequence was previously suggested as one of several mechanisms for the GSH-dependent reduction of human PRDX2 [65]. In contrast to human PRDX2 [65], our measurements do not support a competition between GSH and the resolving cysteinyl residue of the peroxiredoxin for the reduction of the sulfenic acid, since the k_{obs} values for local Tsa1 unfolding and intersubunit disulfide bond formation were not influenced even in the presence of up to 10 mM GSH. The GSH/glutaredoxin system can therefore only serve as a backup system for the thioredoxin system when the yeast thioredoxins are depleted or oxidized. Bolus peroxide treatments of yeast cells could instantaneously oxidize a major fraction of Tsa1. Since the Tsa1 concentration most likely exceeds the concentrations of Trx1 and Trx2 by one or more orders of magnitude [7,12], a single catalytic cycle could completely oxidize the thioredoxin pool. Trx1(S_2) did not react with GSH. Whether the thioredoxins are efficiently reduced again therefore depends on the availability of NADPH and the concentration and activity of thioredoxin reductase. Our glutathione probe responses indicate that thioredoxin reduction can become limiting during bolus peroxide treatments resulting in the Tsa1-and presumably Grx2-dependent formation of GSSG.

In conclusion, we show that Tsa1 is the dominant scavenger of exogenous H_2O_2 and *t*-BuOOH in budding yeast that can become an important source of cytosolic GSSG when the thioredoxin pool becomes oxidized.

4. Materials and methods

4.1. Growth of yeast cells

All experiments in this study were performed in a *Saccharomyces cerevisiae* BY4742 (MATα *his3*Δ1 *leu2*Δ0 *lys2*Δ0 *ura3*Δ0) or YPH499 (*MAT*a *ura3-52 lys2-801_amber ade2-101_ochre trp1-*Δ*63 his3-*Δ*200 leu2-*Δ*1*) background. Cells were grown in Hartwell's Complete (HC) medium with 2 % glucose or a 2 % glycerol/2 % ethanol mixture as carbon sources.

4.2. Construction of yeast strains and plasmid transformation

Most of the yeast gene deletion and gene overexpression strains used here were constructed in previous studies [44,51].For the construction of new yeast gene deletion and overexpression strains a standard homologous recombination-based approach was used [53]. For gene deletion, antibiotic resistance cassettes were amplified by PCR using primers designed to have 50–60 base-pair overhangs homologous to the up- and down-stream regions of the gene to be deleted. Subsequently, the PCR product was transformed into yeast cells using a standard lithium acetate-based protocol. Briefly, cells were harvested and washed with sterile water and resuspended in 200 μl 'One-Step-Transformation' buffer consisting of 40 % (w/v) polyethylene glycol (PEG), 100 mM dithiothreitol (DTT) and 200 mM lithium acetate together with 10 μl salmon sperm DNA and 10 μl PCR product. Cells were incubated at 45 °C for 30 min, transferred to 10 ml of YPD and grown overnight at 30 °C. Cells were subsequently streaked onto YPD plates containing the appropriate antibiotic for selection. Successful gene deletions were confirmed by PCR on genomic DNA using primers designed to bind ~500 bp up- and down-stream of the gene of interest. For genomic DNA extraction, cells were resuspended in 30 μl of 0.2 % (w/v) SDS and heated at 95 °C for 10 min. Subsequently, cells were briefly vortexed and centrifuged at 18000 *g* for 1 min. 2 μl of supernatant was used as template DNA in the PCR reaction mix.

4.3. Cloning and plasmid construction

All genetically encoded probes used in this study were encoded on

p415TEF plasmids. The p415TEF roGFP2-Grx1 [63], roGFP2-Tsa2ΔC$_R$ [44] and Su9-roGFP2-Tsa2ΔC$_R$ [44] were generated in previous studies. HyPer7 was synthesized with codons optimized for yeast expression (Genscript®) and subcloned into an empty p415TEF plasmid using *Xba*I and *Xho*I restriction sites. The p415TEF HyPer7 plasmid was used as a template for mutation of the H_2O_2-reactive cysteine 121 to serine using HyPer7C121S forward primer 5′-CTGAGGGTAACTCTATGAGAGATC-3′ and the HyPer7C121S reverse primer 5′-GATCTCTCATAGAGTTACCCTCAG-3'. Mutation of *C*121 was performed using a standard site-directed mutagenesis protocol using S7-Fusion Polymerase (*Biozym*). Methylated template DNA was digested by *Dpn*I (*NEB*) and 5 μl of the reaction were directly transformed into *E. coli* Top10 cells following plasmid extraction. All plasmids were confirmed by sequencing (Eurofins genomics). Plasmid transformation was performed accordingly. Briefly, cells were harvested, washed and resuspended in 100 μl 'One-Step-Transformation' buffer, followed by the addition of 5 μl salmon sperm DNA and 400 ng plasmid DNA. Cells were then incubated with shaking for 30 min at 45 °C and subsequently streaked onto HC plates lacking leucine for plasmid selection.

4.4. Intracellular H_2O_2 measurements using roGFP2-based redox probes

For Su9-roGFP2-Tsa2ΔC$_R$ measurements, cells were grown in HC media, lacking leucine for plasmid selection with a 2 % (v/v) glycerol/2 % (v/v) ethanol mixture as carbon source. For roGFP2-Tsa2ΔC$_R$ and roGFP2-Grx1 measurements cells were grown in HC media, lacking leucine for plasmid selection with a 2 % glucose (w/v) mixture as carbon source. In all cases, cells were grown at 30 °C with shaking until the culture reached a density of $D \approx 3.5$. Subsequently, cells were resuspended in 100 mM MES/Tris pH 6 buffer to a density of 7.5 D_{600}. Resuspended cells were transferred in 200 μl aliquots to a flat-bottomed 96-well imaging plate (BD Falcon). For every yeast strain measured, one cell aliquot was treated with either 20 mM diamide (*Sigma Aldrich*) and another with 100 mM DTT (*AppChem*) to calibrate full probe oxidation and reduction respectively.

RoGFP2 contains two cysteines located on parallel β-strands adjacent to the chromophore of the GFP. Formation of a disulfide bond between these cysteines induces a change in chromophore protonation and therefore in the excitation spectra. The reduced roGFP2 in its anionic form has a dominant excitation maximum at 488 nm. In contrast, the neutral chromophore in an oxidized roGFP2, exhibits an increased excitation maximum at 400 nm and decreased excitation at 488 nm. Excitation at either 400 or 488 nm leads to fluorescence emission at ~510 nm. The degree of roGFP2 oxidation (OxD) is calculated using the emission intensity at 510 nm following excitation at either 400 nm or 488 nm for the reduced and oxidized controls and the measured sample according to Equation (1).

Equation (1):

$$OxD_{roGFP2} = \frac{(I400sample^{*}I480_{red}) - (I400_{red}{}^{*}I480sample)}{(I400sample^{*}I480_{red} - I400sample^{*}I480_{ox}) + (I400_{ox}{}^{*}I480sample - I400_{red}{}^{*}I480sample)}$$

RoGFP2 fluorescence was followed for ~5 min before the addition of H_2O_2 or *t*-BuOOH. The probe response to the peroxide treatment was followed for ~30 min using a BMG Labtech CLARIOstar fluorescence plate reader. Cells transformed with an empty p415TEF plasmid were used for fluorescence background subtraction.

4.5. Intracellular H_2O_2 measurements using HyPer7

For measurements of HyPer7, cells were grown in HC medium without leucine and 2 % (w/v) glucose as carbon source. In all cases, cells were grown at 30 °C with shaking until the culture reached a density of $D_{600} \approx 1.5$. Subsequently, cells were resuspended in 100 mM MES/Tris pH 6 buffer to a density of 7.5 D_{600}. Resuspended cells were transferred in 200 μl aliquots to a flat-bottomed 96-well imaging plate (BD Falcon). For every yeast strain measured, one cell aliquot was treated with either 1 mM H_2O_2 (*Sigma Aldrich*) and another with 100 mM DTT (*AppChem*) for calibration of the fluorescence plate-reader. HyPer7 is based upon a *circular permutated* yellow fluorescence protein (*cp*YFP) integrated into OxyR domains from *Neisseria meningitidis* [45]. HyPer7 has two fluorescence excitation maxima depending at 410 nm and 490 nm, which are dominant in the reduced and oxidized states respectively. Excitation at either wavelength results in fluorescence emission at 510 nm.

Fluorescence was measured for ~5 min before the addition of H_2O_2 or *t*-BuOOH. The probe response to the peroxide treatment was followed for ~30 min using a BMG Labtech CLARIOstar fluorescence plate reader. Cells transformed with an empty p415TEF plasmid were used for fluorescence background subtraction.

4.6. Purification of recombinant proteins

NADPH was from Gerbu. Diethylenetriaminepentaacetic acid (DTPA), GSH, yeast glutathione reductase (GR), H_2O_2, 3-(dimethylcarbamoylimino)-1,1-dimethylurea (diamide) and 1,4-dithiothreitol (DTT) were from Sigma Aldrich. Plasmids pET15b/ScGrx2 and pET15b/Tsa1 encoding MGSSH$_6$SSGLVPRGSH-tagged Grx2 and Tsa1 were generated by PCR amplification of the coding sequence from pre-existing plasmids, p415 TEF ScGrx2 [74] and p415 TEF roGFP2-Tsa1 [44] using the FWD Grx2 primer catgCATATGGTATCCCAGGAAACAGTTGCTCAC and the REV Grx2 primer ctagCTCGAGctattgaaataccggcttcaatatttcag as well as the FWD Tsa1 Primer catgCATATGGTCGCTCAAGTTCAAAAGCAAGCTCCAAC and the REV Tsa1 primer ctagCTCGAGTTATTTGTTGGCAGCTTC-GAAGTATTCC. Subsequently PCR products were cloned into an empty pET15b using *Nde*I and *Xho*I restriction sites. Please note that the mitochondrial targeting sequence in Grx2 was excluded.

The coding sequence for Trx1 was PCR amplified from yeast genomic DNA using the FWD primer ATGCATCATCACCACCATCACcCCATGGT-TACTCAATTCAAAACTGC and reverse primer cgggtaccgagctcCTC-GAGTTAAGCATTAGCAGCAATGGCTTGC. Subsequently, the PCR product was cloned into an pTrc99a N-6-His vector using *Nco*I and *Xho*I restriction sites. Recombinant Grx2 and Tsa1 were produced in *E. coli* strain SHuffle T7 Express and recombinant Trx1 was produced in *E. coli* strain XL1-Blue. All proteins were purified by Ni-NTA affinity chromatography as described previously for related redoxins [69,75]. Freshly Ni-NTA purified recombinant Tsa1, Grx2 and Trx1 were reduced with 5 mM DTT on ice for 30 min. Excess DTT and imidazole were removed on a PD-10 desalting column (Merck), and the reduced proteins were eluted with 3.5 mL ice-cold assay buffer containing 100 mM $Na_xH_yPO_4$, 0.1 mM DTPA, pH 7.4 (at 25 °C). Reduced Tsa1 or Trx1 was oxidized with 5 mM diamide on ice for 60 min yielding Tsa1(S_2) or Trx1 (S_2). Excess diamide was removed on a Ni-NTA column before the removal of imidazole on a PD-10 column. All enzymes and reactants were diluted/dissolved in ice-cold assay buffer. The purity of all proteins was confirmed by analytical SDS-PAGE. Protein concentrations of the eluates were determined spectrophotometrically using the following extinction coefficients $\varepsilon_{280\ nm}$ as calculated at http://web.expasy.org/

protparam: 23.95 $mM^{-1}cm^{-1}$ for reduced Tsa1, 24.08 $mM^{-1}cm^{-1}$ for oxidized Tsa1, 4.47 $mM^{-1}cm^{-1}$ for reduced Grx2 and 9.97 $mM^{-1}cm^{-1}$ for reduced Trx1. Average yields were 0.4 μmol of recombinant protein per 1 L of *E. coli* culture.

4.7. Stopped-flow kinetic measurements

Recombinant Tsa1, Grx2 and Trx1 were freshly purified, reduced/oxidized and desalted in assay buffer as described above. Stopped-flow measurements were performed at 25 °C in a thermostatted SX-20 spectrofluorometer (Applied Photophysics). The change of tryptophan fluorescence was measured for up to 500 s after mixing (total emission at an excitation wavelength of 295 nm with a slit width of 2 mm). The nonenzymatic reduction of *in situ*-oxidized Tsa1 by GSH was investigated by mixing 2 or 10 μM reduced Tsa1 and variable concentrations of GSH in syringe 1 with 20 or 100 μM H_2O_2 in assay buffer in syringe 2. For the reduction of *in situ*-oxidized Tsa1 by GSH and reduced Grx2, 10 μM reduced Tsa1 with 20 μM reduced Grx2 and variable concentrations of GSH in syringe 1 were mixed with 100 μM H_2O_2 in syringe 2. Alternatively, 10 μM Tsa1(S_2) in syringe 1 was mixed with 20 μM reduced Grx2 and variable concentrations of GSH in syringe 2. The reduction of Tsa1 by Trx1 was measured by mixing 2 μM Tsa1(S_2) in syringe 1 with variable concentrations of reduced Trx1 in syringe 2. The reduction of Trx1 was analyzed by mixing 10 μM Trx1(S_2) in syringe 1 with 20 mM GSH with or without 20 μM reduced Grx2 or 0.8 U/mL GR and 500 μM NADPH in syringe 2. The kinetic traces of three consecutive measurements were averaged and fitted using the Pro-Data SX software (Applied Photophysics). Rate constants k_{obs} from single exponential fits were plotted against the substrate concentration in SigmaPlot 13.0 to obtain second order rate constants from the slopes of the linear fits.

CRediT authorship contribution statement

Jannik Zimmermann: Methodology, Investigation, Formal analysis, Data curation. **Lukas Lang:** Investigation, Formal analysis. **Gaetano Calabrese:** Investigation. **Hugo Laporte:** Investigation. **Prince S. Amponsah:** Investigation. **Christoph Michalk:** Investigation. **Tobias Sukmann:** Investigation. **Julian Oestreicher:** Investigation. **Anja Tursch:** Investigation. **Esra Peker:** Investigation. **Theresa N.E. Owusu:** Investigation. **Matthias Weith:** Investigation. **Leticia Prates Roma:** Writing – review & editing, Writing – original draft, Supervision. **Marcel Deponte:** Writing – review & editing, Writing – original draft, Supervision. **Jan Riemer:** Writing – review & editing, Writing – original draft, Supervision. **Bruce Morgan:** Writing – review & editing, Writing – original draft, Supervision, Funding acquisition, Data curation, Conceptualization.

Declaration of competing interest

The authors declare that they have no conflict of interest.

Acknowledgements

B.M., JR and M.D. acknowledge generous support from the Deutsche Forschungsgemeinschaft (DFG) in the context of Priority Program SPP1710 (MO 2774/2-1, project number 386433891, and DE 1431/8-2 project number 249669453) and grants MO 2774/7-1, project number 508372800, and DE 1431/19-1 project number 508372800) as well as grants RI2150/5-1 project number 435235019, SPP2453 project number 541742459, RTG2550/1 project number 411422114, and CRC1218 - project number 269925409. LPR acknowledges support from the DFG (SFB/TRR219 project number 322900939). The following yeast strains, BY4742 Δ*ccp1*, BY4742 Δ*cta1*Δ*ctt1*, BY4742 Δ*ccp1*Δ*cta1*Δ*ctt1*, BY4742 pRS403, and BY4742 pRS403-*TSA1* were a kind gift from Mikael Molin, Chalmers University of Technology, Gothenburg, Sweden.

Appendix A. Supplementary data

Supplementary data to this article can be found online at https://doi.org/10.1016/j.freeradbiomed.2024.11.004.

References

[1] H. Sies, Role of metabolic H2O2 generation: redox signaling and oxidative stress, J. Biol. Chem. 289 (2014) 8735–8741.
[2] H. Sies, D.P. Jones, Reactive oxygen species (ROS) as pleiotropic physiological signalling agents, Nat. Rev. Mol. Cell Biol. 21 (2020) 363–383.
[3] L. Flohe, S. Toppo, G. Cozza, F. Ursini, A comparison of thiol peroxidase mechanisms, Antioxidants Redox Signal. 15 (2011) 763–780.
[4] S.G. Rhee, I.S. Kil, Multiple functions and regulation of mammalian peroxiredoxins, Annu. Rev. Biochem. 86 (2017) 749–775.
[5] A. Zeida, et al., Catalysis of peroxide reduction by fast reacting protein thiols, Chem. Rev. 119 (2019) 10829–10855.
[6] G. Battistuzzi, M. Bellei, C.A. Bortolotti, M. Sola, Redox properties of heme peroxidases, Arch. Biochem. Biophys. 500 (2010) 21–36.
[7] M. Deponte, The incomplete glutathione puzzle: just guessing at numbers and figures? Antioxidants Redox Signal. 27 (2017) 1130–1161.
[8] M. Molin, et al., Protein kinase A controls yeast growth in visible light, BMC Biol. 18 (2020) 168.
[9] K. Bodvard, et al., Light-sensing via hydrogen peroxide and a peroxiredoxin, Nat. Commun. 8 (2017) 14791.
[10] D. Martins, A.M. English, Catalase activity is stimulated by H(2)O(2) in rich culture medium and is required for H(2)O(2) resistance and adaptation in yeast, Redox Biol. 2 (2014) 308–313.
[11] R. Maslanka, R. Zadrag-Tecza, M. Kwolek-Mirek, Linkage between carbon metabolism, redox status and cellular physiology in the yeast Saccharomyces cerevisiae devoid of SOD1 or SOD2 gene, Genes 11 (2020).
[12] S. Ghaemmaghami, et al., Global analysis of protein expression in yeast, Nature 425 (2003) 737–741.
[13] T. Tachibana, et al., A major peroxiredoxin-induced activation of Yap1 transcription factor is mediated by reduction-sensitive disulfide bonds and reveals a low level of transcriptional activation, J. Biol. Chem. 284 (2009) 4464–4472.
[14] H.Z. Chae, I.H. Kim, K. Kim, S.G. Rhee, Cloning, sequencing, and mutation of thiol-specific antioxidant gene of Saccharomyces cerevisiae, J. Biol. Chem. 268 (1993) 16815–16821.
[15] A.P. Demasi, G.A. Pereira, L.E. Netto, Yeast oxidative stress response. Influences of cytosolic thioredoxin peroxidase I and of the mitochondrial functional state, FEBS J. 273 (2006) 805–816.
[16] I. Iraqui, et al., Peroxiredoxin Tsa1 is the key peroxidase suppressing genome instability and protecting against cell death in Saccharomyces cerevisiae, PLoS Genet. 5 (2009) e1000524.
[17] J. Lu, H. Vallabhaneni, J. Yin, Y. Liu, Deletion of the major peroxiredoxin Tsa1 alters telomere length homeostasis, Aging Cell 12 (2013) 635–644.
[18] C.M. Wong, K.L. Siu, D.Y. Jin, Peroxiredoxin-null yeast cells are hypersensitive to oxidative stress and are genomically unstable, J. Biol. Chem. 279 (2004) 23207–23213.
[19] M.E. Huang, A.G. Rio, A. Nicolas, R.D. Kolodner, A genomewide screen in Saccharomyces cerevisiae for genes that suppress the accumulation of mutations, Proc. Natl. Acad. Sci. U. S. A. 100 (2003) 11529–11534.
[20] C.M. Grant, G. Perrone, I.W. Dawes, Glutathione and catalase provide overlapping defenses for protection against hydrogen peroxide in the yeast Saccharomyces cerevisiae, Biochem. Biophys. Res. Commun. 253 (1998) 893–898.
[21] J. Lee, D. Spector, C. Godon, J. Labarre, M.B. Toledano, A new antioxidant with alkyl hydroperoxide defense properties in yeast, J. Biol. Chem. 274 (1999) 4537–4544.
[22] Y. Inoue, T. Matsuda, K. Sugiyama, S. Izawa, A. Kimura, Genetic analysis of glutathione peroxidase in oxidative stress response of Saccharomyces cerevisiae, J. Biol. Chem. 274 (1999) 27002–27009.
[23] J.R. Pedrajas, A. Miranda-Vizuete, N. Javanmardy, J.A. Gustafsson, G. Spyrou, Mitochondria of Saccharomyces cerevisiae contain one-conserved cysteine type peroxiredoxin with thioredoxin peroxidase activity, J. Biol. Chem. 275 (2000) 16296–16301.
[24] A.M. Avery, S.V. Avery, Saccharomyces cerevisiae expresses three phospholipid hydroperoxide glutathione peroxidases, J. Biol. Chem. 276 (2001) 33730–33735.
[25] M.K. Cha, et al., Nuclear thiol peroxidase as a functional alkyl-hydroperoxide reductase necessary for stationary phase growth of Saccharomyces cerevisiae, J. Biol. Chem. 278 (2003) 24636–24643.
[26] A.M. Avery, S.A. Willetts, S.V. Avery, Genetic dissection of the phospholipid hydroperoxidase activity of yeast gpx3 reveals its functional importance, J. Biol. Chem. 279 (2004) 46652–46658.
[27] D. Greetham, C.M. Grant, Antioxidant activity of the yeast mitochondrial one-Cys peroxiredoxin is dependent on thioredoxin reductase and glutathione in vivo, Mol. Cell Biol. 29 (2009) 3229–3240.
[28] D.E. Fomenko, et al., Thiol peroxidases mediate specific genome-wide regulation of gene expression in response to hydrogen peroxide, Proc. Natl. Acad. Sci. U. S. A. 108 (2011) 2729–2734.
[29] S. Stocker, K. Van Laer, A. Mijuskovic, T.P. Dick, The conundrum of hydrogen peroxide signaling and the emerging role of peroxiredoxins as redox relay hubs, Antioxidants Redox Signal. 28 (2018) 558–573.

[30] H.H. Jang, et al., Two enzymes in one; two yeast peroxiredoxins display oxidative stress-dependent switching from a peroxidase to a molecular chaperone function, Cell 117 (2004) 625–635.
[31] F. Teixeira, et al., Mitochondrial peroxiredoxin functions as crucial chaperone reservoir in Leishmania infantum, Proc. Natl. Acad. Sci. U. S. A. 112 (2015) E616–E624.
[32] F. Ursini, et al., Dual function of the selenoprotein PHGPx during sperm maturation, Science 285 (1999) 1393–1396.
[33] F. Roger, et al., Peroxiredoxin promotes longevity and H_2O_2-resistance in yeast through redox-modification of protein kinase A, bioRxiv (2019).
[34] G. Calabrese, et al., Hyperoxidation of mitochondrial peroxiredoxin limits H2 O2 -induced cell death in yeast, EMBO J. 38 (2019) e101552.
[35] A.M. Day, et al., Inactivation of a peroxiredoxin by hydrogen peroxide is critical for thioredoxin-mediated repair of oxidized proteins and cell survival, Mol. Cell 45 (2012) 398–408.
[36] D. Greetham, et al., Oxidation of the yeast mitochondrial thioredoxin promotes cell death, Antioxidants Redox Signal. 18 (2013) 376–385.
[37] A. Domenech, J. Ayte, F. Antunes, E. Hidalgo, Using in vivo oxidation status of one- and two-component redox relays to determine H(2)O(2) levels linked to signaling and toxicity, BMC Biol. 16 (2018) 61.
[38] R.M. Jarvis, S.M. Hughes, E.C. Ledgerwood, Peroxiredoxin 1 functions as a signal peroxidase to receive, transduce, and transmit peroxide signals in mammalian cells, Free Radic. Biol. Med. 53 (2012) 1522–1530.
[39] K.H. Koo, et al., Regulation of thioredoxin peroxidase activity by C-terminal truncation, Arch. Biochem. Biophys. 397 (2002) 312–318.
[40] T.S. Chang, et al., Regulation of peroxiredoxin I activity by Cdc2-mediated phosphorylation, J. Biol. Chem. 277 (2002) 25370–25376.
[41] H.A. Woo, et al., Inactivation of peroxiredoxin I by phosphorylation allows localized H(2)O(2) accumulation for cell signaling, Cell 140 (2010) 517–528.
[42] E.A. Veal, Z.E. Underwood, L.E. Tomalin, B.A. Morgan, C.S. Pillay, Hyperoxidation of peroxiredoxins: gain or loss of function? Antioxidants Redox Signal. 28 (2018) 574–590.
[43] M.N. Hoehne, et al., Spatial and temporal control of mitochondrial H(2) O(2) release in intact human cells, EMBO J. 41 (2022) e109169.
[44] B. Morgan, et al., Real-time monitoring of basal H2O2 levels with peroxiredoxin-based probes, Nat. Chem. Biol. 12 (2016) 437–443.
[45] V.V. Pak, et al., Ultrasensitive genetically encoded indicator for hydrogen peroxide identifies roles for the oxidant in cell migration and mitochondrial function, Cell Metabol. 31 (2020) 642–653 e6.
[46] I.A. Calvo, et al., Dissection of a redox relay: H2O2-dependent activation of the transcription factor Pap1 through the peroxidatic Tpx1-thioredoxin cycle, Cell Rep. 5 (2013) 1413–1424.
[47] A. Delaunay, D. Pflieger, M.B. Barrault, J. Vinh, M.B. Toledano, A thiol peroxidase is an H2O2 receptor and redox-transducer in gene activation, Cell 111 (2002) 471–481.
[48] B. Morgan, M.C. Sobotta, T.P. Dick, Measuring E(GSH) and H2O2 with roGFP2-based redox probes, Free Radic. Biol. Med. 51 (2011) 1943–1951.
[49] V. Staudacher, et al., Redox-sensitive GFP fusions for monitoring the catalytic mechanism and inactivation of peroxiredoxins in living cells, Redox Biol. 14 (2018) 549–556.
[50] P.S. Amponsah, et al., Peroxiredoxins couple metabolism and cell division in an ultradian cycle, Nat. Chem. Biol. (2021).
[51] S. Hanzen, et al., Lifespan control by redox-dependent recruitment of chaperones to misfolded proteins, Cell 166 (2016) 140–151.
[52] K. Kim, I.H. Kim, K.Y. Lee, S.G. Rhee, E.R. Stadtman, The isolation and purification of a specific "protector" protein which inhibits enzyme inactivation by a thiol/Fe (III)/O2 mixed-function oxidation system, J. Biol. Chem. 263 (1988) 4704–4711.
[53] C. Janke, et al., A versatile toolbox for PCR-based tagging of yeast genes: new fluorescent proteins, more markers and promoter substitution cassettes, Yeast 21 (2004) 947–962.
[54] Y. Ogura, Catalase activity at high concentration of hydrogen peroxide, Arch. Biochem. Biophys. 57 (1955) 288–300.
[55] R.K. Bonnichsen, B. Chance, H. Theorell, Catalase activity, Acta Chem. Scand. 1 (1947) 685–709.
[56] L.C. Seaver, J.A. Imlay, Alkyl hydroperoxide reductase is the primary scavenger of endogenous hydrogen peroxide in Escherichia coli, J. Bacteriol. 183 (2001) 7173–7181.
[57] J. Kunkel, X. Luo, A.P. Capaldi, Integrated TORC1 and PKA signaling control the temporal activation of glucose-induced gene expression in yeast, Nat. Commun. 10 (2019) 3558.
[58] M. Johnston, A model fungal gene regulatory mechanism: the GAL genes of Saccharomyces cerevisiae, Microbiol. Rev. 51 (1987) 458–476.
[59] D.B. Berry, A.P. Gasch, Stress-activated genomic expression changes serve a preparative role for impending stress in yeast, Mol. Biol. Cell 19 (2008) 4580–4587.
[60] P. Kritsiligkou, T.K. Shen, T.P. Dick, A comparison of Prx- and OxyR-based H2O2 probes expressed in S. cerevisiae, J. Biol. Chem. 100866 (2021).
[61] A. Zhuravlev, et al., HyPer as a tool to determine the reductive activity in cellular compartments, Redox Biol. 70 (2024) 103058.
[62] S. Ragu, et al., Loss of the thioredoxin reductase Trr1 suppresses the genomic instability of peroxiredoxin tsa1 mutants, PLoS One 9 (2014) e108123.
[63] B. Morgan, et al., Multiple glutathione disulfide removal pathways mediate cytosolic redox homeostasis, Nat. Chem. Biol. 9 (2013) 119–125.
[64] M. Deponte, Glutathione catalysis and the reaction mechanisms of glutathione-dependent enzymes, Biochim. Biophys. Acta 1830 (2013) 3217–3266.
[65] A.V. Peskin, et al., Glutathionylation of the active site cysteines of peroxiredoxin 2 and recycling by glutaredoxin, J. Biol. Chem. 291 (2016) 3053–3062.
[66] M. Gutscher, et al., Real-time imaging of the intracellular glutathione redox potential, Nat. Methods 5 (2008) 553–559.
[67] C.A. Tairum, et al., Catalytic thr or ser residue modulates structural switches in 2-cys peroxiredoxin by distinct mechanisms, Sci. Rep. 6 (2016) 33133.
[68] A. Kriznik, et al., Dynamics of a key conformational transition in the mechanism of peroxiredoxin sulfinylation, ACS Catal. 10 (2020) 3326–3339.
[69] L. Lang, et al., Substrate promiscuity and hyperoxidation susceptibility as potential driving forces for the Co-evolution of Prx5-type and Prx6-type 1-Cys peroxiredoxin mechanisms, ACS Catal. 13 (2023) 3627–3643.
[70] S.F. Villar, et al., Kinetic and structural assessment of the reduction of human 2-Cys peroxiredoxins by thioredoxins, FEBS J. 291 (2024) 778–794.
[71] S. Luikenhuis, G. Perrone, I.W. Dawes, C.M. Grant, The yeast Saccharomyces cerevisiae contains two glutaredoxin genes that are required for protection against reactive oxygen species, Mol. Biol. Cell 9 (1998) 1081–1091.
[72] E. Eckers, M. Bien, V. Stroobant, J.M. Herrmann, M. Deponte, Biochemical characterization of dithiol glutaredoxin 8 from Saccharomyces cerevisiae: the catalytic redox mechanism redux, Biochemistry 48 (2009) 1410–1423.
[73] L. Liedgens, M. Deponte, The catalytic mechanism of glutaredoxins, in: L. Flohe (Ed.), Glutathione, Taylor & Francis Inc, 2018, pp. 251–262.
[74] J. Zimmermann, et al., One cysteine is enough: a monothiol Grx can functionally replace all cytosolic Trx and dithiol Grx, Redox Biol. 36 (2020) 101598.
[75] F. Geissel, L. Lang, B. Husemann, B. Morgan, M. Deponte, Deciphering the mechanism of glutaredoxin-catalyzed roGFP2 redox sensing reveals a ternary complex with glutathione for protein disulfide reduction, Nat. Commun. 15 (2024) 1733.
[76] C.C. Winterbourn, D. Metodiewa, Reactivity of biologically important thiol compounds with superoxide and hydrogen peroxide, Free Radic. Biol. Med. 27 (1999) 322–328.
[77] H. Ostergaard, C. Tachibana, J.R. Winther, Monitoring disulfide bond formation in the eukaryotic cytosol, J. Cell Biol. 166 (2004) 337–345.
[78] C.C. Winterbourn, The biological chemistry of hydrogen peroxide, Methods Enzymol. 528 (2013) 3–25.
[79] M. Deponte, C.H. Lillig, Enzymatic control of cysteinyl thiol switches in proteins, Biol. Chem. 396 (2015) 401–413.
[80] L. van Dam, et al., The human 2-Cys peroxiredoxins form widespread, cysteine-dependent- and isoform-specific protein-protein interactions, Antioxidants 10 (2021).
[81] R.D.M. Travasso, F. Sampaio Dos Aidos, A. Bayani, P. Abranches, A. Salvador, Localized redox relays as a privileged mode of cytoplasmic hydrogen peroxide signaling, Redox Biol. 12 (2017) 233–245.
[82] C.C. Winterbourn, Reconciling the chemistry and biology of reactive oxygen species, Nat. Chem. Biol. 4 (2008) 278–286.
[83] J.B. Lim, B.K. Huang, W.M. Deen, H.D. Sikes, Analysis of the lifetime and spatial localization of hydrogen peroxide generated in the cytosol using a reduced kinetic model, Free Radic. Biol. Med. 89 (2015) 47–53.
[84] Y. Goulev, et al., Nonlinear feedback drives homeostatic plasticity in H2O2 stress response, Elife 6 (2017).
[85] N.M. Mishina, et al., Does cellular hydrogen peroxide diffuse or act locally? Antioxidants Redox Signal. 14 (2011) 1–7.
[86] N.M. Mishina, et al., Which antioxidant system shapes intracellular H2O2 gradients? Antioxidants Redox Signal. 31 (2019) 664–670.
[87] E. Paulo, et al., A genetic approach to study H2O2 scavenging in fission yeast–distinct roles of peroxiredoxin and catalase, Mol. Microbiol. 92 (2014) 246–257.
[88] D. Talwar, J. Messens, T.P. Dick, A role for annexin A2 in scaffolding the peroxiredoxin 2-STAT3 redox relay complex, Nat. Commun. 11 (2020) 4512.
[89] J.M. Lim, K.S. Lee, H.A. Woo, D. Kang, S.G. Rhee, Control of the pericentrosomal H2O2 level by peroxiredoxin I is critical for mitotic progression, J. Cell Biol. 210 (2015) 23–33.
[90] S. Mishra, J. Imlay, Why do bacteria use so many enzymes to scavenge hydrogen peroxide? Arch. Biochem. Biophys. 525 (2012) 145–160.
[91] L.C. Seaver, J.A. Imlay, Hydrogen peroxide fluxes and compartmentalization inside growing Escherichia coli, J. Bacteriol. 183 (2001) 7182–7189.
[92] M.C. Sobotta, et al., Peroxiredoxin-2 and STAT3 form a redox relay for H2O2 signaling, Nat. Chem. Biol. 11 (2015) 64–70.
[93] S. Stocker, M. Maurer, T. Ruppert, T.P. Dick, A role for 2-Cys peroxiredoxins in facilitating cytosolic protein thiol oxidation, Nat. Chem. Biol. 14 (2018) 148–155.
[94] J.A. Imlay, Pathways of oxidative damage, Annu. Rev. Microbiol. 57 (2003) 395–418.
[95] J.A. Imlay, The molecular mechanisms and physiological consequences of oxidative stress: lessons from a model bacterium, Nat. Rev. Microbiol. 11 (2013) 443–454.
[96] F. Roger, et al., Peroxiredoxin promotes longevity and H2O2-resistance in yeast through redox-modulation of protein kinase A, Elife 9 (2020).
[97] M.D. Pineyro, T. Arcari, C. Robello, R. Radi, M. Trujillo, Tryparedoxin peroxidases from Trypanosoma cruzi: high efficiency in the catalytic elimination of hydrogen peroxide and peroxynitrite, Arch. Biochem. Biophys. 507 (2011) 287–295.
[98] M. Trujillo, et al., Pre-steady state kinetic characterization of human peroxiredoxin 5: taking advantage of Trp84 fluorescence increase upon oxidation, Arch. Biochem. Biophys. 467 (2007) 95–106.
[99] R. Schumann, L. Lang, M. Deponte, Characterization of the glutathione-dependent reduction of the peroxiredoxin 5 homolog PfAOP from Plasmodium falciparum, Protein Sci. 31 (2022) e4290.